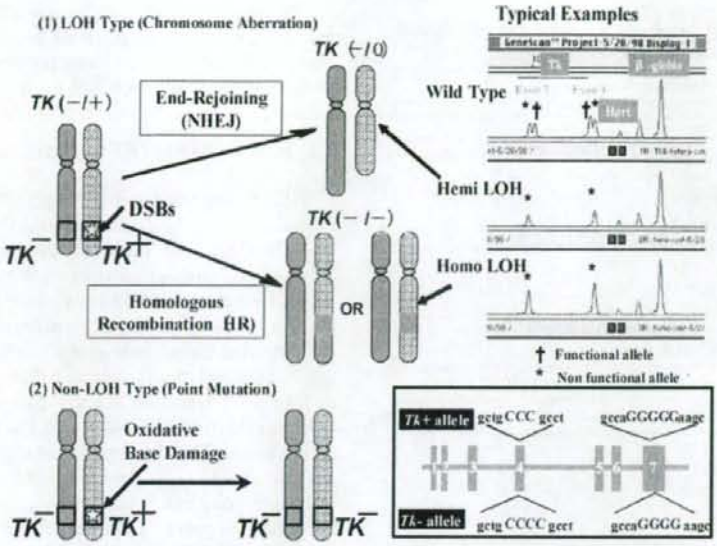

Fig. 1. LOH classifications of TK^- mutants. The first step in the genetic analysis of selected TK^- mutants was to judge whether there was a loss of *TK* heterozygosity (LOH). This was accomplished by PCR amplification of exons 4 and 7 regions of the *TK* locus. This step also distinguished between hemizygous LOH (loss of the functional *TK* allele) and homozygous LOH (replacement of the functional *TK* allele by a mutated TK^- allele (see ref. [29]).

as a "non-LOH" mutant. We used the same technique to distinguish between hemizygous LOH (in which the functional *TK* allele is lost) and homozygous LOH (in which the functional *TK* allele is replaced by TK^-). To determine the extent and size of the deleted or substituted portions of the chromosome involved, we analyzed 11 microsatellite regions (D17S588, D17S1784, D17S785, D17S789, D17S802, D17S807, D17S928, D17S932, D17S1299, D17S1566 and THRA) on chromosome 17 using multiple PCR reactions as described previously [29]. The fine structure of the recovered TK^- LOH mutations was determined by chromosome mapping analysis.

2.5. Base sequencing of non-LOH mutants

For a precise analysis of non-LOH mutants, we extracted RNA using Isogen (Nippon Gene, Japan), and obtained cDNA using a First-Strand cDNA Synthesis Kit, Amersham, USA). Following PCR amplification, the purified 807-bp fragments were sequenced by Takara Bio (Japan). The primers 5′-AGAGTACTCGGGTTCGTGAA-3′ and 5′-GCAGCATGCAGGGCAGCGTG-3′ (forward and reverse, respectively) were used for cDNA synthesis, PCR amplification and base sequencing [30]. To prevent the overestimation of mutational events, we counted identical mutations originating from a single irradiated dish as a single event.

Table 1a
TK mutation frequency (MF) at various time intervals between priming and challenging X-ray exposures (priming dose, 10 cGy; challenging dose, 2 Gy)

Time interval (h)	0	1.5	3	6	9	12
TK MF ($\times 10^{-6}$)	19.8	18.1	14.4	13.5	17.8	19.7

3. Results

3.1. Optimum conditions for mutagenic adaptation

For inducing an adaptive response to X-ray irradiation, the optimum interval between a 10-cGy priming dose and a 2-Gy challenging dose was 6 h (Table 1a), and the optimum priming dose 6 h prior to a 2-Gy challenging dose was 5 cGy (Table 1b). We therefore decided to characterize the induced *TK* mutants by repeating

Table 1b
TK mutation frequency at various priming X-ray doses (challenging dose, 2 Gy; interval between 2 exposures, 6 h)

Priming X-ray dose (cGy)	0	2.5	5	10
TK MF ($\times 10^{-6}$)	13.3	15.8	4.5	6.3

Table 2
Surviving fractions of primed and non-primed TK6 cells following challenge exposure to 2 Gy X-rays

Experiment	Surviving fraction	
	Non-primed cells	Primed cells (5 cGy)
I	0.043	0.047
II	0.047	0.070
III	0.049	0.040
Mean ± S.D.	0.046 ± 0.0031*	0.052 ± 0.016*

* $P = 0.58$; t-test.

Table 3
TK mutation frequency in primed and non-primed TK6 cells following challenge exposure to 2 Gy X-rays

Experiment	*TK* mutation frequencies ($\times 10^{-6}$)	
	Non-primed cells	Primed cells (5 cGy)
I	13.3	4.5
II	13.3	10.5
III-a	20.4	15.1
III-b	21.0	15.6
Mean ± S.D.	18.3 ± 4.3*	11.4 ± 5.1*

Experiments III-a and III-b were carried out concurrently with survival assay III, but they were independent mutation assays.
* $P = 0.020$; t-test.

our mutation experiments under those conditions (5 cGy followed 6 h later with 2 Gy).

3.2. Survival assay and TK mutation assay

Table 2 shows the surviving fraction, expressed as PE (2 Gy X-ray irradiated cells)/PE (unirradiated cells) of primed and unprimed cells immediately after the 2-Gy challenge exposure. Irradiation with the priming dose of 5 cGy did not influence the PE of unchallenged cells (data not shown). The effect of priming on survival after 2 Gy X-ray irradiation was 1.1 (0.052/0.046; $P = 0.58$, t-test). Thus, priming did not significantly affect survival after the challenge exposure.

On the other hand, priming did affect the *TK* MF induced by the challenge. Data from 4 independent experiments showed that priming reduced the MF to 62% of the unprimed MF ($P = 0.020$, t-test) (Table 3).

3.3. LOH analysis of TK^- mutants

Table 4 shows the distributions of LOH classes among the isolated TK^- mutants as determined by PCR analysis. We isolated non- and "small" LOH mutants (see Sections 3.4 & 3.5) as normal growth mutants in the first selection, except for a few cases. We isolated the remaining LOH mutants as slow growth mutants in the second selection. We estimated the pre-exposure effect from the proportion of each mutational event as follows: (i) 7.1×10^{-6} to 1.9×10^{-6} reduction in corresponding MF of non-LOH events, (ii) 6.4×10^{-6} to 6.1×10^{-6} change in corresponding MF of hemizygous LOH events and (iii) 5.1×10^{-6} to 3.1×10^{-6} reduction in corresponding MF of homozygous LOH events. Thus, the MF of a non-LOH event in primed cells was reduced to 27% of the non-primed MF. The induction of hemizygous events, on the other hand, was barely influenced by priming. As far as homozygous events go, their corresponding MF was reduced to 61% of the original level, which was similar to level of reduction in total MF (62%).

3.4. Analysis of LOH tracts on chromosome 17

Fig. 2 shows the deleted or replaced regions of chromosome 17 in each LOH mutant. Mutants reflected both type 1 and type 2 LOH events. Type 1 defines a terminal event; that is, the deleted or exchanged chromosome segment extends to the telomere marker (D17S928). Type 2 defines an interstitial deletion; the altered segment does not reach the telomere marker.

In the present study, most hemizygous LOH mutations, which are considered to be the result of DSB non-homologous end-joining (NHEJ) repair, reflected

Table 4
Distribution of mutational classes among the isolated *TK* mutants

Mutational class	Number of identified mutants (Exp. I, II, III-a, III-b) [MF $\times 10^{-6}$]	
	Non-primed cells	Primed cells (5 cGy)
Non-LOH	18 (5, 4, 6, 3) [7.1]	8 (1, 3, 2, 2) [1.9]
LOH		
Hemizygous	15 (3, 3, 7, 2) [6.0]	27 (8, 7[a], 5, 7) [6.4]
Homozygous	13 (3, 4, 3, 3) [5.1]	13 (2, 3, 5, 3) [3.1]
Total	46 (11, 11, 16, 8) [18.3]	48 (11, 13, 12, 12) [11.4]

[a] One of the seven mutants was a mixed hemizygous/homozygous type.

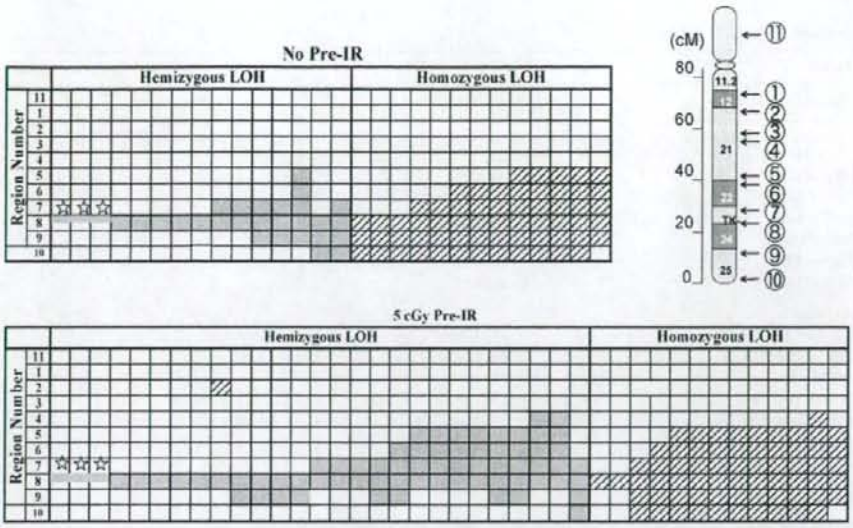

Fig. 2. Chromosome mapping of the LOH mutants. We analyzed the LOH mutants selected after a 2 Gy of challenging X-ray irradiation to determine the extent of the deleted or exchanged portions of the chromosome. The upper panel shows the profiles of 28 LOH mutants selected from non-primed cells, and the lower panel shows the profiles of 40 LOH mutants selected from cells primed with 5 cGy of X-rays. Each column represents a single LOH mutant. The rows represent regions of chromosome 17 diagrammed in the upper right insert. Shaded squares represent deleted regions and hatched squares represent exchanged regions (see text). The region numbers refer to the 11 microsatellite regions: (1) D17S588; (2) D17S1784; (3) D17S785; (4) D17S789; (5) D17S802; (6) D17S807; (7) D17S928; (8) D17S932; (9) D17S1299; (10) D17S1566; (11) THRA (see ref. [29]). The star symbol represents a "small" type 2 hemizygous event in which the deletion is restricted to *TK* locus.

type 2 events in both the non-primed (13 of 15 mutants) and primed (26 of 27 mutants) groups. Small type 2 deletions – those restricted to the *TK* locus (Fig. 2) – were infrequent in both groups (3 of 15 mutants in non-primed cells and 3 of 27 in primed cells). Similarly, the proportion of large deletion mutants (expanding to the region beyond region 8, Fig. 2) was also similar in the primed (18 of 27 mutants) and non-primed (7 of 15 mutants) groups. Homozygous LOH events, on the other hand, which are considered to be the result of homologous recombination (HR) repair of DSBs, were primarily identified as type 1 events in both primed (10 of 13) and non-primed (12 of 13) groups. Interestingly, small homozygous LOH events (where only a single region was replaced, Fig. 2) were recovered from the primed cells (2 of 13 (3 0f 14)), but not from the non-primed cells (0 of 13).

3.5. Analysis of non-LOH-mutants

We detected many types of alterations in the non-LOH mutant cDNAs (Table 5). The proportion of single base-substitutions among all the mutations identified as this class was 1/8 (13%) in the primed cells, and this value was clearly lower than 7/18 (87%) in the unprimed cells. G and C bases were targeted in base substitution mutations, except for a single case of an A to T transversion (Table 5). Most (4/5) of the double-base changes consisted of a single base deletion (causing a frameshift) and a base substitution, except for a single case of a GC to TA double transversion in a radioadapted mutant. It is difficult to estimate the effect of priming on the induction of the double-base change events from the limited number of cells involved. Similar difficulties were also found in the other mutational events in this class such as triple-base changes, multiple-base changes and exon skipping. In addition, the proportion of abnormal transcription events (both functional and non-functional *TK* alleles are equally transcribed) was also similar in the radioadapted (1/8, 13%) and the non-adapted (3/18, 17%) group, although its origin was not identified.

4. Discussion

The radioadaptation conditions used in this study (5 cGy of priming X-rays followed in 6 h by 2 Gy of challenging X-rays) were similar to those used in other studies [4,6,11,12,14,16]. The *TK* mutation frequency

Table 5
Nature of the isolated non-LOH mutants

Type of mutation		Number of identified mutants	
Specific changes	[Position: exon]	Non-primed exposure	Primed (5 cGy) pre-X-ray
Single base substitutions		7	1
G → A (Gly → Glu)	[56:1]	3	0
C → T (Gln → Stop)	[64:1]	1	0
C → A (Ser → Stop)	[89:2]	1	0
A → T (Ser → Cys)	[97:2]	1	0
G → C (Leu → Phe)	[108:2]	0	1
G → A (Glu → Lys)	[430:6]	1	0
Double base changes		3	2
G → A (Gly → Glu)/Del. C	[56:1/676:7]	1	0
G → C (Leu → Phe)/Del. A	[108:2/686:7]	0	1
Add. C/Del. G	[232:4/641:7]	1	0
GC → TA (Leu Asp → Leu Asn)	[372 and 373:5]	0	1
G → A (Glu → Lys)/Del. G	[430:6/447:6]	1	0
Triple base changes		0	1
Del. G/C → T (Ile → Ile)/C → T (Leu → Leu)	[92:1/288:4/561:7]	0	1
Multiple base changes		1	1
CC → AT (Thr Gln → Thr Stop)/G → A (Gln → Gln)/G → A (Gln → Gln)/Add. C/Del. G	[51 and 52:1/66:1/667:7/232:4/641:7]	0	1
Base changes at 20 sites		1	0
Exon skipping, abnormal splicing and deletion		3	2
Del. of a part of exon 1 (48 bases)	[161–209: 1]	1	1
Abnormal splicing of intron (between exons 1 and 2)		1	0
Skipping of exon 3 (Del. 111 bases)	[99–203: 3]	1	0
Skipping of exon 5 (Del. 90 bases)	[304–393: 5]	0	1
Abnormal transcription		3	1
Both functional and non-functional alleles are equally transcribed			
Unidentified		1	0
Total		18	8

we observed after the challenge X-rays (18.3×10^{-6}) was reduced by the 5-cGy priming exposure to about 62% of the non-primed level (11.4×10^{-6}). Taking into consideration the *TK* spontaneous mutation frequency observed in our recent study (3.0×10^{-6}) [32], the increase in MF induced by 2 Gy of X-rays was reduced from 6.1-fold to 3.8-fold.

We originally planned this study to determine whether radioadaptation would alter the characteristics of X-ray-induced LOH events. X-ray-induced interstitial deletions are likely to be the result of NHEJ repair of DSBs, and this type of mutation was the one we recovered most frequently after 2 Gy X-ray irradiation in our previous study [24]. We also found that carbon-ion beam irradiation induced interstitial deletions more efficiently than the same dose of X-rays [26,27], which we interpreted as the result of a higher occurrence of inaccurately repaired DSBs. In the present study, however, we found that the frequency of hemizygous LOH mutations, as well as their size and the distribution of deleted regions on chromosome 17, was similar for radioadapted and non-adapted cells. Those results are not consistent with reports suggesting that enhanced repair of DSBs reduces chromosomal alterations [21,22]. An entire genome assay might lead to results similar to the ones in those reports, but our observations were restricted to the *TK* locus on chromosome 17.

On the other hand, we observed a decrease in the induction of homozygous LOH events in the primed cells, which suggests that priming enhanced the HR repair of DSBs. We recently constructed a model system to follow the fate of a single DSB introduced by the restriction enzyme I-sceI at a specific site in the *TK* gene in TK6 cells [31]. In preliminary exper-

iments, low dose/low-dose rate γ-irradiation (30 mGy at 1.2 mGy/h) did not significantly affect end joining (EJ) repair of this specific DSB, but it enhanced the efficiency of HR repair by about 50% (unpublished data). The small homozygous LOH events we observed in the primed cells in the present study (3/14) might reflect this enhanced HR, but we must examine whether the adaptive response was really involved because we also recovered small homozygous LOH mutants after the low-dose/low-dose rate γ-ray exposures [32]. The decrease in the frequency of single-base substitutions that we observed in primed cells (1/48) versus non-primed cells (7/46) (Tables 4 and 5) is rarely influenced by counting base substitutions accompanied by single base deletions (which would result in 2/48 for primed cells and 9/46 for non-primed cells), so the most likely mechanism for the reduced induction of non-LOH mutants was suppression of base substitutions.

One of the possible targets for radioadaptation is oxidative base damage. In fact, down-regulation of the human *CDC16* gene that occurs after oxidative stress causes more rapid and efficient repair in adapted (2 cGy pre-irradiated) human lymphoblastoid cells challenged with 4 Gy irradiation [6]. On the other hand, oxidative base excision repair enzymes, including DNA glycosylases, hOGG1 and hNth1, are reportedly not up-regulated at the post-transcriptional level in γ-ray-primed TK6 cells [33]. Since DNA glycosylase can suppress base substitution, we need to examine whether radioadaptation enhances the enzyme's activity under the present condition. Alternatively, base substitution activity might not accurately reflect DNA glycosylase activity because attempted base excision repair of IR damage by the enzyme can lead to lethal and mutagenic DSBs [34].

A variety of untargeted effects may contribute to the short- and long-term fate of a cell exposed to IR [35]. An example is the possible involvement of a "radioadaptive bystander" effect in human lung fibroblasts [36]. The reduction of radiosensitivity in cells with a wild type *p53* gene by a radiation-induced, nitric oxide (NO)-mediated bystander effects may be a manifestation of the radioadaptive response [37,38]. This possibility is supported by the finding that the NO-induced apoptosis observed in lymphoblastoid and fibroblast cells depends on the phosphorylation and activation of p53 [39]. However, it is still unclear whether the NO-mediated pathway also contributes to the mutagenic adaptation. The de novo protein synthesis is required for expression of adaptive responses [22,40], and gene expression studies are improving our understanding of the molecular mechanisms underlying the radioadaptive response [9,10,40,41]. Our laboratory is also focusing on the molecular mechanisms involved in radioadaptation, especially the expression of genes involved in DNA base and nucleotide excision repair.

Acknowledgements

This study was partially supported by the Budget for Nuclear Research of the Ministry of Education, Culture, Sports, Science and Technology, and was reviewed by the Atomic Energy Commission of Japan. We thank Dr. Miriam Bloom (SciWrite Biomedical Writing & Editing Services) for professional editing.

References

[1] G. Olivieri, Y. Bodycote, S. Wolf, Adaptive response of human lymphocytes to low concentrations of radioactive thymidine, Science 223 (1984) 594–597.
[2] S. Wolf, Aspects of the adaptive response to very low doses of radiation and other agents, Mutat. Res. 358 (1996) 135–142.
[3] S. Wolf, The adaptive response in radiobiology: evolving insights and implications, Environ. Health Pesrpect. 106 (1998) 277–283.
[4] O. Rigaud, E. Moustacchi, Radioadaptation for gene mutation and the possible molecular mechanisms of the adaptive response, Mutat. Res. 358 (1996) 127–134.
[5] M. Wojewodska, M. Kruzewski, K. Iwanenko, I. Szumiel, Effects of signal transduction in adapted lymphocytes: micronuclei frequency and DNA repair, Int. J. Radiat. Biol. 71 (1997) 245–252.
[6] P.-K. Zhou, O. Rigaud, Down-regulation of the human *CDC16* gene after exposure to ionizing radiation: a possible role in the radioadaptive response, Radiat. Res. 155 (2001) 43–49.
[7] M.S. Sasaki, Y. Ejima, A. Tachibana, T. Yamada, K. Ishizaki, T. Shimizu, T. Nomura, DNA damage response pathway in radioadaptive response, Mutat. Res. 504 (2002) 101–118.
[8] I. Szumiel, Adaptive responses: stimulated DNA repair or decreased damage fixation? Int. J. Radiat. Biol. 81 (2005) 233–241.
[9] M.A. Coleman, E. Yin, L.E. Peterson, D. Nelson, K. Sorensen, J.D. Tucker, A.J. Wyrobeck, Low-dose irradiation alters the transcript profiles of human lymphoblastoid cells inducing genes associated with radioadaptive response, Radiat. Res. 164 (2005) 369–382.
[10] H.P. Wang, X.H. Long, Z.Z. Sun, O. Rigaud, Q.Z. Xu, Y.C. Huang, J.L. Sui, B. Bai, P.K. Zhou, Identification of differentially transcribed genes in human lymphoblastoid cells irradiated with 0.5 Gy of γ-ray and the involvement of low dose radiation inducible CHD6 gene in cell proliferation and radiosensitivity, Int. J. Radiat. Biol. 82 (2006) 181–190.
[11] S.G. Swant, G. Randers-Pehrson, N.F. Metting, E.J. Hall, Adaptive response and the bystander effect induced by radiation in C3H 10T1/2 cells in culture, Radiat. Res. 156 (2001) 177–180.
[12] H.N. Zhou, G. Randers-Pehrson, C.R. Geard, D.J. Brenner, E.J. Hall, T.K. Hei, Interaction between radiation-induced adaptive response and bystander mutagenesis in mammalian cells, Radiat. Res. 160 (2003) 512–516.
[13] W.M. Bonner, Thresholds, bystander effect, and adaptive response, Proc. Natl. Acad. Sci. U.S.A. 100 (2003) 4973–4975.
[14] S.A. Mitchell, S.A. Marino, D.J. Brenner, E.J. Hall, Bystander effect and adaptive response in C3H 10T(1/2) cells, Int. J. Radiat. Biol. 80 (2004) 465–472.

[15] T.K. Hei, R. Persaud, H. Zhou, M. Suzuki, Genotoxicity in the eyes of bystander cells, Mutat. Res. 568 (2004) 111–120.
[16] T. Ikushima, Chromosomal response to ionizing radiation reminiscent of an adaptive response in cultured Chinese hamster cells, Mutat. Res. 180 (1987) 215–221.
[17] B.J.S. Sanderson, A.A. Morely, Exposure of human lymphocytes to ionizing radiation reduces mutagenicity by subsequent radiation, Mutat. Res. 164 (1986) 151–347.
[18] P.K. Zhou, X.Y. Liu, W.Z. Sun, Y.P. Zhang, Y.P.K. Wei, Cultured mouse SR-1 cells exposed to low-dose of γ-rays become less susceptible to the induction of mutations by radiation as well as bleomycin, Mutagenesis 8 (1993) 109–111.
[19] A.M. Ueno, D.B. Vannais, S.L. Gustafson, J.C. Wong, C.A. Waldren, A low adaptive dose of gamma-rays reduced the number and altered the spectrum of S1 mutants in human hamster hybrid cells, Mutat. Res. 358 (1996) 161–169.
[20] E.I. Azzam, G.P. Raaphorst, R.E. Mitchel, Radiation-induced adaptive response for protection against micronucleus formation and neoplastic transformation in C3H 10T1/2 mouse embryo cells, Radiat. Res. 138 (1994) S28–S31.
[21] O. Rigaud, D. Papadopoulo, E. Moustacchi, Decreased deletion mutation in radioadapted human lymphoblast, Radiat. Res. 133 (1993) 94–101.
[22] T. Ikushima, H. Aritomi, J. Morisita, Radioadaptive response: efficient repair of radiation-induced DNA damage in adapted cells, Mutat. Res. 358 (1996) 193–198.
[23] T.R. Skopek, H.L. Liber, B.W. Penman, W.G. Thilly, Isolation of a human lymphoblastoid line heterozygous at the thymidine kinase locus: possibility for a rapid human cell mutation assay, Biochem. Biophys. Res. Commun. 84 (1978) 411–416.
[24] M. Honma, M. Hayashi, T. Sofuni, Cytotoxic and mutagenic responses to X-rays and chemical mutagens in normal and p53-mutated human lymphoblastoid cell, Mutat. Res. 374 (1996) 89–98.
[25] M. Honma, L.S. Zhang, M. Hayashi, K. Takeshita, Y. Nakagawa, N. Tanaka, T. Sofuni, Illegitimate recombination leading to allelic loss and unbalanced translocation in p53-mutated human lymphoblastoid cells, Mol. Cell. Biol. 17 (1997) 4774–4781.
[26] S. Morimoto, T. Kato, M. Honma, M. Hayashi, F. Hanaoka, F. Yatagai, Detection of genetic alterations induced by low-dose X rays: analysis of loss of heterozygosity for *TK* mutation in human lymphoblastoid cells, Radiat. Res. 157 (2002) 533–538.
[27] S. Morimoto, M. Honma, F. Yatagai, Sensitive detection of LOH events in a human cell line after C-ion beam exposure, J. Radiat. Res. 43 (Suppl.) (2002) S163–S167.
[28] Y. Umebayashi, M. Honma, T. Abe, H. Ryuto, H. Suzuki, T. Shimazu, N. Ishioka, M. Iwaki, F. Yatagai, Mutation induction after low-dose carbon-ion beam irradiation of frozen human cultured cells, Biol. Sci. Space 19 (2005) 237–241.
[29] F. Yatagai, S. Morimoto, T. Kato, M. Honma, Further characterization of loss of heterozygosity enhanced by p53 abrogation in human lymphoblastoid TK6 cells: disappearance of endpoint hotspots, Mutat. Res. 560 (2004) 133–145.
[30] A.J. Grosvsky, B.N. Walter, C.R. Giver, DNA-sequence specificity of mutations at the human thymidine kinase locus, Mutat. Res. 289 (1993) 231–243.
[31] M. Honma, M. Izumi, M. Sakuraba, S. Tadokoro, H. Sakamoto, W. Wang, F. Yatagai, M. Hayashi, Deletion, rearrangement, and gene conversion; genetic consequences of chromosomal double-strand breaks in human cells, Environ. Mol. Mutagen. 42 (2003) 288–298.
[32] Y. Umebayashi, M. Honma, M. Suzuki, H. Suzuki, T. Shimazu, N. Ishioka, M. Iwaki, F. Yatagai, Mutation induction in cultured human cells after low-dose and low-dose-rate γ-ray irradiation: detection by LOH analysis, J. Radiat. Res. 48 (2006) 7–11.
[33] M. Inoue, G.-P. Shen, M.A. Chaudhry, H. Galick, J.O. Blaisdell, S.S. Wallace, Expression of the oxidative base excision repair enzymes is not induced in TK6 human lymphoblastoid cells after low doses of ionizing radiation, Radiat. Res. 161 (2004) 409–417.
[34] N. Yang, H. Galick, S.S. Wallace, Attempted base excision repair of ionizing radiation damage in human lymphoblastoid cells produces lethal and mutagenic double-strand breaks, DNA Repair 3 (2004) 1323–1334.
[35] P.J. Coates, S.A. Lorimore, E.G. Wright, Damaging and protective cell signaling in the untargeted effects of ionizing radiation, Mutat. Res. 568 (2004) 5–20.
[36] R. Iyer, B.E. Lehnert, Low-dose, low-LET ionizing radiation-induced radioadaptation and associated early responses in unirradiated cells, Mutat. Res. 503 (2002) 1–9.
[37] H. Matsumoto, A. Takahashi, T. Ohnishi, Radiation-induced adaptive and bystander effects, Biol. Sci. Space 18 (2004) 247–254.
[38] H. Matsumoto, A. Takahashi, T. Ohnishi, Nitric oxide radicals choreograph a radioadaptive response, Cancer Res. 67 (2007) 8574–8579.
[39] L.M. McLaughlin, B. Demple, Nitric oxide-induced apoptosis in lymphoblastoid and fibroblast cells dependent on the phosphorylation and activation of p53, Cancer Res. 65 (2005) 6097–6104.
[40] J.H. Yongblom, J.K. Wiencke, S. Wolf, Inhibition of the adaptive response of human lymphocytes to very low doses of ionizing radiation by the protein synthesis inhibitor cycloheximide, Mutat. Res. 227 (1989) 257–261.
[41] L.-H. Ding, M. Shingyoji, F. Chen, J.-J. Hwang, S. Burma, C. Lee, J.-F. Chen, D.J. Chen, Gene expression profiles of normal human fibroblasts after exposure to ionizing radiation: a comparative study of low and high doses, Radiat. Res. 164 (2005) 17–26.

Mutation Research 673 (2009) 9–20

Contents lists available at ScienceDirect

Mutation Research/Genetic Toxicology and Environmental Mutagenesis

journal homepage: www.elsevier.com/locate/gentox
Community address: www.elsevier.com/locate/mutres

Dose-dependent alterations in gene expression in mouse liver induced by diethylnitrosamine and ethylnitrosourea and determined by quantitative real-time PCR☆

Takashi Watanabe[a], Gotaro Tanaka[b], Shuichi Hamada[c], Chiaki Namiki[d], Takayoshi Suzuki[e], Madoka Nakajima[f], Chie Furihata[a,*]

[a] Functional Genomics Laboratory, School of Science and Engineering, Aoyama Gakuin University, Fuchinobe 5-10-1, Sagamihara, Kanagawa 229-0006, Japan
[b] Tokushima Research Center, Taiho Pharmaceutical Co. Ltd., Hiraishiebisuno 224-2, Kawauchichou, Tokushima, Tokushima 771-0194, Japan
[c] Genetic Toxicology Group, Toxicology Division II, Kashima Laboratory, Mitsubishi Chemical Safety Institute Ltd., Sunayama 14, Kamisu-shi, Ibaraki 314-0255, Japan
[d] Central Research Laboratory, SSP Co. Ltd., Nanpeidai 1143, Narita, Chiba 286-8511, Japan
[e] Division of Cellular & Gene Therapy Products, National Institute of Health Sciences, Kamiyoga 1-18-1 Setagaya-ku, Tokyo 158-8501, Japan
[f] Genetic Toxicology Group, Biosafety Research Center, Foods, Drugs, and Pesticides, Shioshinden 582-2, Fukude-cho, Iwata-gun, Shizuoka 437-1213, Japan

ARTICLE INFO

Article history:
Received 29 September 2008
Received in revised form 31 October 2008
Accepted 9 November 2008
Available online 21 November 2008

Keywords:
Genotoxic carcinogens
Dose-dependent alteration
Hierarchical clustering
k-means clustering
IPA

ABSTRACT

We examined the dose-dependency of gene expression changes for 51 genes in mouse liver treated with two *N*-nitroso genotoxic hepatocarcinogens, diethylnitrosamine (DEN) and ethylnitrosourea (ENU) by quantitative real-time PCR (qPCR). DEN (3, 9, 27 and 80 mg/kg bw) or ENU (6, 17, 50 and 150 mg/kg bw) was injected intraperitoneally into groups of five male 9-week-old B6C3F$_1$ mice and the livers were dissected after 4 h and 28 days. Total RNA from pooled livers was reverse-transcribed to cDNA and the amount of each gene was quantified by qPCR. Results were analyzed by hierarchical and *k*-means clustering and ingenuity pathway analysis (IPA). The most characteristic result was a similar dose-dependency of gene expression changes with DEN and ENU. Twenty-one genes exhibited a distinct dose-dependent increase in expression at 4 h for both carcinogens [*Bax*, *Btg2*, *Ccng1*, *Cdkn1a*, *Cyp4a10*, *Cyp21a1*, *Fos*, *Gadd45b*, *Gdf15*, *Hmox1*, *Hspb1*, *Isg20l1*, *Jun*, *Mbd1*, *Mdm2*, *Myc*, *Net1*, *Plk2*, *Ppp1r3c*, *Rcan1* and *Tubb2c*], although the increase in gene expression due to ENU was generally weaker than that due to DEN. Only *Gdf15* showed a dose-dependent increase in expression at 28 days for both carcinogens. The differences between DEN and ENU were in the expression of additional genes (7 for DEN and 8 for ENU). IPA extracted five gene networks: Network-1 included genes related to cancer and cell cycle arrest and associated with *Bax*, *Btg2*, *Ccng1*, *Cdkn1a*, *Gadd45b*, *Gdf15*, *Hspb1*, *Mdm2* and *Plk2* and Network-2 was related to DNA replication, recombination, repair and cell death and associated with *Cyp21a1*, *Gdf15*, *Ppp1r3c*, *Rcan1* and *Tubb2c*. The present results show a distinct dose-dependency of gene expression changes induced by DEN and ENU. These changes were associated with cancer, cell cycle arrest, DNA replication, recombination, repair and cell death and were seen not only at 4 h but also, for some, at 28 days after administration.

1. Introduction

Diethylnitrosamine (DEN) and ethylnitrosourea (ENU) are potent genotoxic *N*-nitroso carcinogens that induce hepatocellular carcinomas in mouse liver [1,2]. It has been reported that after its metabolic biotransformation, DEN produces the promutagenic adducts O^6-ethylguanine (O^6-EtG) and O^4- and O^2-ethylthymine and that O^4-ethylthymine may be responsible for the initiation of hepatocellular carcinomas in rats [3]. ENU, which is a direct-ethylating agent, forms several major adducts upon reaction with DNA, of which O^6-EtG, O^4- and O^2-ethylthymine and N^3-ethylthymine have been implicated in mutagenic lesions [4]. Suzuki et al. have reported that mutagenic activity by DEN and ENU was clearly detected with the *lacZ* mutation assay in mouse liver at 7 days [5]. Mientjes et al. have reported that the O^6-EtG levels increased as early as 1.5 h after treatment, whereas at 3 days more than 90% of the lesions had been removed from the DNA in the livers of DEN- and ENU-treated mice, based on *lacZ* transgenic mice [6]. After this period, however, with the bulk of O^6-EtG removed, the induction of *lacZ* mutations was observed at 3 days and continued to increase for some weeks.

☆ This work was a JEMS/MMS/Toxicogenomics group collaborative study.

* Corresponding author at: Department of Chemistry and Biological Science, School of Science and Engineering, Aoyama Gakuin University, 5-10-1 Fuchinobe, Sagamihara, Kanagawa 229-8558, Japan. Tel.: +42 759 6233; fax: +42 759 6511.
E-mail address: chiefurihata@gmail.com (C. Furihata).

1383-5718/$ – see front matter © 2008 Elsevier B.V. All rights reserved.
doi:10.1016/j.mrgentox.2008.11.004

Previously, Waring et al. showed by DNA microarray that a number of genes are up-regulated and down-regulated in rat liver, with rats dosed daily with DEN for 3 days and euthanized on the 4th day [7]. Genes up-regulated by DEN included genes related to growth arrest and DNA damage, such as *Bax*, *Ccnd1*, *Ccng1*, *Cdkn1a/p21*, *Gadd45* and *Jun*. However, no studies have focused on either the DNA damaging time of 4 h or the mutation fixing time of 28 days in DEN-treated mouse or rat liver. Although it has been reported that ENU induced expression of *Bax*, *Crp*, *Cyp2a*, *Gstm2*, *Icam1*, *Mig*, and *Mt2* mRNA in mouse liver, little is known about differential gene expression in ENU-exposed rodent liver [8].

Quantitative real-time PCR (qPCR) is an alternative technology for toxicogenomics [9]. qPCR is a highly regarded and reliable quantitative method but analysis of a large number of genes may be lengthy. It is impractical to examine a great number of genes with qPCR. Therefore, we selected 51 candidate genes (Table 1) based on our previous results using the Affymetrix GeneChip Mu74AV2 and original DNA microarray to determined the effects of DEN, dimethylnitrosamine, dipropylnitrosamine, ENU, *o*-aminoazotoluene, 7,12-dimethylbenz[*a*]anthracene, dibenzo[*a*,*l*]pyrene, phenobarbital and ethanol exposure in mouse liver for 4 and 20 h and 14 and 28 days in our JEMS/MMS/Toxicogenomics group collaborative study; results were reported in part [10]. We examined gene expression changes at an early time after administration, as we were interested in whether toxicogenomics was useful for carcinogen screening. In the previous study, using a single dose for each chemical, gene expression changes in number and degree were observed to peak at 4 h after administration. It is known that genotoxic *N*-nitroso carcinogens induce DNA damage and repair in a matter of a few hours after their administration; DNA adducts [6], DNA strand-breaks [11], unscheduled DNA synthesis [12] and other lesions have been reported. It is also known that mutations are observed in transgenic mouse liver 28 days after genotoxic *N*-nitroso carcinogen administration [5,6]. However, related gene expression changes at these time points have not yet been fully elucidated.

Table 1
Fifty-one genes examined in the present study.

No.	Symbol	Gene name	Accession number
1	*Bax*	Bcl2-associated X protein	NM_007527
2	*Bcl2*	B-cell leukemia/lymphoma 2	NM_009741
3	*Btg2*	B-cell translocation gene 2, anti-proliferative	NM_007570
4	*Casp1*	IL-1B converting enzyme; interleukin 1 beta-converting enzyme	NM_009807
5	*Ccnf*	Cyclin F	NM_007634
6	*Ccng1*	Cyclin G1	NM_009831
7	*Ccng2*	Cyclin G2	NM_007635
8	*Cdkn1a (p21)*	Cyclin-dependent kinase inhibitor 1A (P21)	NM_007669
9	*Cyp1a1*	Cytochrome P450, family 1, subfamily a, polypeptide 1	NM_009992
10	*Cyp1a2*	Cytochrome P450, family 1, subfamily a, polypeptide 2	NM_009993
11	*Cyp4a10*	Cytochrome P450, family 4, subfamily a, polypeptide 10	NM_010011
12	*Cyp21a1*	Cytochrome P450, family 21, subfamily a, polypeptide 1	NM_009995
13	*Dpyd*	Dihydropyrimidine dehydrogenase	NM_170778
14	*Egfr*	Epidermal growth factor receptor	NM_207655
15	*Ephx1*	Epoxide hydrolase 1, microsomal	NM_010145
16	*Fabp5*	Fatty acid binding protein 5, epidermal	NM_010634
17	*Fos*	FBJ osteosarcoma oncogene	NM_010234
18	*Gadd45b*	Growth arrest and DNA-damage-inducible 45 beta	NM_008655
19	*Gadd45g*	Growth arrest and DNA-damage-inducible 45 gamma	NM_011817
20	*Gapdh*	Glyceraldehyde-3-phosphate dehydrogenase	NM_008084
21	*Gdf15*	Growth differentiation factor 15	NM_011819
22	*Glul*	Glutamate-ammonia ligase (glutamine synthetase)	NM_008131
23	*Gstk1*	Glutathione S-transferase kappa 1	NM_029555
24	*Gyk*	Glycerol kinase	NM_212444
25	*Hist1h1c*	H1 histone family, member 2	NM_015786
26	*Hspa1b (Hsp70)*	Heat shock protein 1B	NM_010478
27	*Hspb1*	Heat shock protein 1	NM_013560
28	*Hspb2 (Hsp27)*	Heat shock protein 2	NM_024441
29	*Hmox1*	Heme oxygenase (decycling) 1	NM_010442
30	*Hprt1*	Hypoxanthine guanine phosphoribosyl transferase 1	NM_013556
31	*Igfbp1*	Insulin-like growth factor binding protein 1	NM_008341
32	*Isg20l1*	Interferon stimulated exonuclease gene 20-like 1	NM_026531
33	*Jun*	Jun oncogene	NM_010591
34	*Kras*	v-Ki-ras2 Kirsten rat sarcoma viral oncogene homolog	NM_021284
35	*Lig3*	Ligase III, DNA, ATP-dependent	NM_010716
36	*Lrp1*	Low density lipoprotein receptor-related protein 1	NM_008512
37	*Mbd1*	Methyl-CpG binding domain protein 1	NM_013594
38	*Mdm2*	Transformed mouse 3T3 cell double minute 2	NM_010786
39	*Myc*	Myelocytomatosis oncogene	NM_010849
40	*Net1*	Neuroepithelial cell transforming gene 1	NM_019671
41	*Pdgfb*	Platelet-derived growth factor, B polypeptide	NM_011057
42	*Plk2*	Polo-like kinase 2; serum-inducible kinase	NM_152804
43	*Pml*	Promyelocytic leukemia	NM_008884
44	*Pmm1*	Phosphomannomutase 1	NM_013872
45	*Ppp1r3c*	Protein phosphatase 1, regulatory (inhibitor) subunit 3C	NM_016854
46	*Rad52*	RAD52 homolog (S. cerevisiae)	NM_011236
47	*Rcan1(Dscr1)*	Regulator of calcineurin 1	NM_019466
48	*Trp53*	Transformation related protein 53	NM_011640
49	*Tubb2c*	Tubulin, beta 2c	NM_146116
50	*Ube2e1 (UbcM3)*	Ubiquitin-conjugating enzyme E2E 1, UBC4/5 homolog (yeast)	NM_009455
51	*Ung*	Uracil-DNA glycosylase	NM_011677

In this paper, we report our studies of gene expression changes in B6C3F$_1$ mouse liver induced by multiple doses of two typical alkylating agents, DEN and ENU. We investigated the dose-dependency of gene expression changes at two different time points: 4 h, characterized by the production of many DNA lesions, and 28 days, characterized by fixing of mutations [6]. If we could show dose-dependency in gene expression changes at 4 h, we could clarify key genes related to DNA lesions and subsequent various phenomena in liver cells induced by DEN and ENU. If we could show the dose-dependency in gene expression changes at 28 days, we could clarify key genes related to effects of mutations and subsequent changes that may be causal for carcinogenesis. Our purpose is to determine biological cell responses induced by DEN and ENU by examining the dose-dependency at these two time points.

In addition, we examined gene networks using IPA to elucidate interactions between genes with altered expression.

2. Materials and methods

2.1. Animal treatment

Male B6C3F$_1$ mice were obtained at 8 weeks of age from Charles River Japan, Inc. (Yokohama, Japan). They were kept in plastic cages on wood chips as bedding and given food (Oriental MF, Oriental Yeast Co., Tokyo) and water *ad libitum* in an air-conditioned room [12 h light (7 a.m. to 7 p.m.), 12 h dark; 23 ± 2 °C; 55 ± 5% humidity]. All animal experiments were conducted in accordance with the NIH Guide for Care and Use of Laboratory Animals and approved by the Animal Care and Use Committee at the Mitsubishi Chemical Safety Institute Ltd.

Mice at 9 weeks of age were injected intraperitoneally (i.p.) with DEN (3, 9, 27 and 80 mg/kg bw; Wako Pure Chem. Ind. Ltd., Osaka, Japan; CAS 55-18-5) dissolved in sterile water or ENU (6, 17, 50 and 150 mg/kg bw; Wako Pure Chem. Ind. Ltd., Osaka, Japan; CAS 759-73-9) dissolved in sterile water. Control animals for the DEN- and ENU-treated groups received sterile water. At 4 h and 28 days after treatment, animals were sacrificed after which the liver was collected, frozen on dry ice, and stored at −80 °C until use.

2.2. RNA isolation and relative quantification by real-time PCR

To isolate total RNA, approximately 150 mg from each liver (main lobe) was placed into TRIzol reagent (Invitrogen Corp., Carlsbad, CA, USA) and immediately homogenized using a Potter homogenizer. The samples were further homogenized with a 1 ml syringe and 18 gauge needle. Finally, total RNA was purified using an ethanol precipitation method. Complementary DNA (cDNA) was yielded from total RNA using the SuperScript First strand synthesis system for RT-PCR kit (Invitrogen Corp.).

qPCR amplifications were performed in triplicate using the SYBR Green I assay in an Opticon II (MJ Research, Inc., Waltham, MA, USA). The reactions were carried out in a 96-well plate in 20-μl reactions containing 2× SYBR Green Master Mix (Applied Biosystems, Lincoln Centre Drive Foster City, CA, USA), 2 pmol each of forward and reverse primer, and a cDNA template corresponding to 10 ng total RNA. Each primer sequence and Ct value are shown in Table 2. We selected 51 genes based on our previous results from the original DNA microarray and Affymetrix GeneChip Mu74AV2 for samples after treatment of DEN, dimethylnitrosamine, dipropylnitrosamine, ENU, o-aminoazotoluene, 7,12-dimethylbenz[*a*]anthracene, dibenzo[*a,l*]pyrene, phenobarbital and ethanol in our JEMS/MMS/Toxicogenomics group collaborative study. *Gapdh* and *Hprt1* were selected as housekeeping genes. SYBR Green PCR conditions were 95 °C for 10 min, followed by 95 °C for 10 s, 58 °C for 50 s and 72 °C for 20 s, for 45 cycles. In each assay a standard curve was determined concurrently with examined samples. In the preliminary experiment the highest group was selected for each gene and was used as the standard sample in the subsequent assay. In each standard curve determination, there were six dilution series of standard samples, diluted up to 1/5, 1/25, 1/125, 1/625 and 1/3125 of the selected standard liver cDNA for each gene. Finally, relative quantitative values of each sample were determined with 1/25 diluted cDNA and were normalized with those of the *Gapdh* genes. Relative *Gapdh* expression levels of experimental groups are presented in Fig. 1.

2.3. Data analysis and clustering algorithm

For the cluster analysis program, we performed a logarithmic ($\log_2$) transformation of the data to stabilize the variance and the gene expression profile of each DEN- and ENU-treated sample, normalized to the median gene expression level for the entire sample set. Both hierarchical and *k*-means clustering were performed using GENESIS software (http://genome.tugraz.at/) [13] for each data set at 4 h and 28 days separately. Gene groups were presented automatically by hierarchical clustering. Four clusters were set up initially in *k*-means clustering based on hierarchical clustering results. Genes which belonged to dose–response groups by both clustering methods were defined as dose–response genes. Furthermore, genes which showed less than a 0.5-fold decrease dose-dependently were evaluated as decrease genes by expression pattern because the decrease genes were few and could not be extracted using both clustering methods.

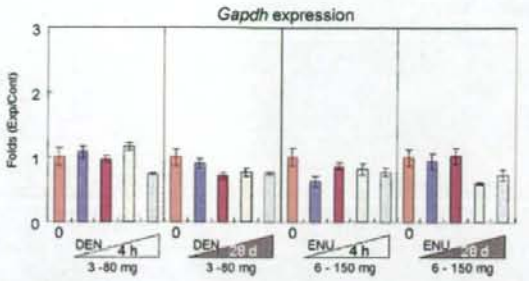

Fig. 1. Relative expression of *Gapdh*. DEN (0–80 mg/kg bw) and ENU (0–150 mg/kg bw) were given to 9-week-old mice (five per group). Total RNA was extracted from pooled liver and reverse-transcribed to cDNA. *Gapdh* expression was determined by qPCR in triplicate assays. Results are shown as mean ± S.D.

The color displays given in Fig. 2 show the $\log_2$ (expression ratio) as (1) red when the treatment sample is up-regulated relative to the control sample, (2) blue when the treatment sample is down-regulated relative to the control sample and (3) white when the $\log_2$ (expression ratio) is close to zero.

2.4. Pathway analysis

Numerical experimental data at 4 h and 28 days after DEN or ENU treatment were separately analyzed by ingenuity pathway analysis (IPA) Software-Complete Pathways Database. These data were generated through the use of IPA, a web-delivered application (www.Ingenuity.com) that enables the visualization and analysis of biologically relevant networks to discover, visualize, and explore therapeutically relevant networks. IPA information was extracted by experts from the full text of the scientific literature, including information about genes, drugs, chemicals, cellular and disease processes, and signaling and metabolic pathways.

Expression data sets containing gene identifiers (Entrez gene identifiers) and their corresponding expression values as fold changes were uploaded as a tab-delimited text file. Each gene identifier was mapped to its corresponding gene object in the Ingenuity Pathways Knowledge Base. To start building networks, the application program queries the Ingenuity Pathways Knowledge Base for interactions between focus genes and all other gene objects stored in the knowledge base and generates a set of networks. The program then computes a score for each network according to the fit of the network to the set of focus genes. The score indicates the likelihood of the focus genes in a given network being found together due to random chance. A score of >2 indicates that there is a <1 in 100 chance that the focus genes were assembled randomly into a network due to random chance.

3. Results

3.1. Dose-dependent alteration of gene expression induced by DEN

3.1.1. Clustering analysis for gene expression

Unsupervised hierarchical clustering results are shown in Fig. 2. The changes in gene expression are represented colorimetrically as described in Section 2. The clustering presented four groups (DEN-4 h-Grp-1 to DEN-4 h-Grp-4) and an ungrouped gene 4 h after administration, and three groups (DEN-28 d-Grp-1 to DEN-28 d-Grp-3) and eight ungrouped genes 28 days after administration. As unsupervised hierarchical clustering was performed for 4 h and 28-day samples separately, group member genes were different for 4 h groups and 28-day groups.

At 4 h, all 20 DEN-4 h-Grp-1 genes showed a dose-dependent increase of more than 3–64-fold. Twelve DEN-4 h-Grp-2 genes were suggested to have a gradual dose-dependent increase of less than that for the expression in DEN-4 h-Grp-1. Two DEN-4 h-Grp-4 genes exhibited a dose-dependent decrease of less than 0.3-fold.

Table 2
Primer sequences of 51 genes examined in the study.

No.	Symbol	Left	Right	Ct
1	*Bax*	CCAGGATGCGTCCACCAAGAAG	GGAGTCCGTGTCCACGTCAGC	28
2	*Bcl2*	GATGACTTCTCTCGTCGCTACC	CATCCCTGAAGAGTTCCTCCAC	31
3	*Btg2*	ACGGGAAGAGAACCGACATGC	ATGATCGGTCAGTGCGTCCTG	24
4	*Casp1*	GTCTTGGAGACATCCTGTCAGG	GCATCTGTAGCCTAAATTCTGG	32
5	*Ccnf*	AGCACAAAGCCTTGCCACCATC	AAGCCAGGTGCGTGTCCTTGTC	25
6	*Ccng1*	TGGCCGAGATTTGACCTTCTGG	GTGCTTCAGTTGCCGTGCAGTG	22
7	*Ccng2*	GCCATCAAGCTAGGACTGTTAG	CACTTATCAACTCCATTCCCTG	26
8	*Cdkn1a (p21)*	TCCCCTGGACAGTGAGCAGTTG	CGTCTCCGTGACGAAGTCAAAG	22
9	*Cyp1a1*	TGGCCGATCGGAGGTCTTTC	AAGTGTTCACAGCGGGCGTG	29
10	*Cyp1a2*	GATGCTCTTCGGCTTGGGAAAG	CCATAGTTGGGTGTCAGGTCCAC	20
11	*Cyp4a10*	AGCCACAAGGGCAGTGTTCAGG	CCAAGCGGCCATTGGAAGAAAG	23
12	*Cyp21a1*	TGTGCTGCCCTTAAAGAAGAGTG	TTGAGCATCCCGTTCCCGTTTC	25
13	*Dpyd*	GTGCGGCTAAAGGCTGATGTGG	CCCATGGTTCACTGGTTTGCATG	24
14	*Egfr*	AGAACGCCTTCCACAGCCAC	ACTCTCGGAACTTTGGGCGG	22
15	*Ephx1*	CATTGTCTCCTCCCAGCGCTTC	GGGCATGCAGGATCTCAGAAGG	21
16	*Fabp5*	ACGGTCTGCACCTTCCAAGACG	ACCCGAGTGCAGGTGGCATTG	24
17	*Fos*	GTCGACCTAGGGAGGACCTTAC	CATCTCTGGAAGAGGTGAGGAC	31
18	*Gadd45b*	TGTACGAGGCGGCCAAACTG	TGTCGCAGCAGAACGACTGG	28
19	*Gadd45g*	GGAAAGCACAGCCAGGATGCAG	ATTCAGGACTTTGGCGGACTCG	26
20	*Gapdh*	GCTCTCAATGACAACTTTGTCAAG	CTTCCTTGGAGGCCATGTAGGC	22
21	*Gdf15*	AGCTGGAACTGCGCTTACGGG	CTCCAGCCCAAGTCTTCAAGAG	28
22	*Glul*	GGAATGGAGCAGGAATATACTC	ACCGCAGTAATACGGGCCTTG	22
23	*Gstk1*	CGTACTCCTGGCTGGGGCTTTG	CAGGTGGTTGGTTGCCGCTGTC	24
24	*Gyk*	GCCTGAAACAACTGCACTAGGC	CACAGCTTTCTTCCATGTGGAG	27
25	*Hist1h1c*	CGAGCTCATCACCAAGGCTGTG	CCCTTGCTCACCAGGCTCTTC	26
26	*Hspa1b (Hsp70)*	GACAAGTCGGAGAACGTGCAG	CGAGTAGGTGGTGAAGGTCTG	25
27	*Hspb1*	CGGTGCTTCACCCGGAAATAC	GCTGACTGCGTGACTGCTTTGG	25
28	*Hspb2 (Hsp27)*	CTCACAGTGAAGACCAAGGAAG	GGATAGGGAAGAGGACACTAGG	26
29	*Hmox1*	AAGACCGCCTTCCTGCTCAAC	CGAAGTGACGCCATCTGTGAGG	28
30	*Hprt1*	CTTGCTCGAGATGTCATGAAGGAG	TAATCCAGCAGGTCAGCAAAGAAC	26
31	*Igfbp1*	GATCAGCCCATCCTGTGGAACG	TTCTCGTTGGCAGGGCTCCTTC	24
32	*Isg20l1*	TTGAAGGGCAAGGTGGTGGTG	GAGCAGGTTTGGGACATAAGTG	24
33	*Jun*	GCCAAGAACTCGGACCTTCTC	AGTGGTGATGTGCCCATTGCTG	23
34	*Kras*	GGCAAGAGCGCCTTGACGATAC	TGGTCCCTCATTGCACTGTACTCC	28
35	*Lig3*	TGCGGCTCTACTTGCCACCTTC	CATGTGTGGCTGAGCCCATGTC	27
36	*Lrp1*	GGGCCATGAATGTGGAAATTGG	GTGGCATACACTGGGTTGGTG	22
37	*Mbd1*	GGATCCTGACACTCAAGAATGG	GTTTGGGCTAACACAGGAAGAG	23
38	*Mdm2*	TTGATCCGAGGCTGGGTCTGTG	AAGATCCTGATGCGAGGGCGTC	27
39	*Myc*	B5,6TCAGCAACAACCGCAAGTGCTC	AAAGCTGCGCTTCAGCTCGTTC	32
40	*Net1*	GACCTCCACGAAGAGTGTGAAG	CTGTACACTGGAGCCACAATCC	27
41	*Pdgfb*	AAGACGCGCACAGAGGTGTTCC	GGCATTGCACATTGCGGTTATTG	33
42	*Plk2*	CTGTTGAGAGCGTCTTCAGTTG	CCATAGTTCACAGTTAAGCAGC	28
43	*Pml*	GGCAAGAAGCGTCCTTACCTTC	GGACAGCAACAGCAGTTCAGTC	28
44	*Pmm1*	TGTCCCGAGGAGGCATGATAAG	CAAAGTCATTCCCGCCAGGAC	30
45	*Ppp1r3c*	TGGAAACCTGACGGAGTGCAG	GCAAGCCTTGGACTGCCAAAG	24
46	*Rad52*	TGACGCCACTCACCAGAGGAAG	GCTGGAAGTACCGCATGCTTGG	30
47	*Rcan1*	GGTCCACGTGTGTGAGAGTG	TGGATGGGTGTGTACTCCGG	24
48	*Trp53*	TTGGACCCTGGCACCTACAATG	GCAGACAGGCTTTGCAGAATGG	26
49	*Tubb2c*	TTGGCAACAGCACCGCTATTC	TCGGACACCAGGTCGTTCATG	23
50	*Ube2e1 (UbcM3)*	AACTGGAGCCCAGCCCTAACC	TGGCCATTCTGTCGTGTTCTGC	24
51	*Ung*	AACCTGAGTGGCCTCGTCTTCC	TCTGCATCCCAGGAACCCTCTG	29

Ct values are those of the highest group in the present experimental condition.

At 28 days, three DEN-28 d-Grp-1 genes showed a dose-dependent increase of more than four-fold. Seventeen DEN-28 d-Grp-2 genes were suggested to have a gradual dose-dependent increase, though less than that for the expression in DEN-28 d-Grp-1. Ungrouped *Igfbp1* showed a dose-dependent decrease of less than 0.3-fold.

Unsupervised *k*-means clustering results are shown in Fig. 3A. Genes were classified into four clusters based on the hierarchical clustering results. Gene expression was classified into four clusters (DEN-4 h-Cluster-1 to DEN-4 h-Cluster-4) 4 h after administration, and four clusters (DEN-28 d-Cluster-1 to DEN-28 d-Cluster-4) 28 days after administration. As unsupervised *k*-means clustering was performed for 4 h and 28-day data separately, cluster member genes were different for 4 h and 28 days.

At 4 h, all 12 DEN-4 h-Cluster-1 genes exhibited a dose-dependent increase of more than eight-fold. Fourteen DEN-4 h-Cluster-2 genes showed a gradual dose-dependent increase as compared to DEN-4 h-Cluster-1 genes. Although *Myc* and *Igfbp1* in DEN-4 h-Cluster-3 had some atypical dose–response, they showed an increase of up to or greater than two-fold, as a whole. Two genes in DEN-4 h-Cluster-4 exhibited a dose-dependent decrease of less than 0.3-fold [*Cyp1a2* and *Glul*]. For 28-day data, 4 DEN-28 d-Cluster-1 genes showed a dose-dependent increase of more than two-fold. *Igfbp1* in DEN-28 d-Cluster-3 showed a dose-dependent decrease of less than 0.3-fold.

Two types of clustering results for the DEN data are summarized as follows. A total of 28 genes showed a dose-dependent increase or decrease at 4 h or 28 days after administration. Twenty-six genes in DEN-4 h-Grp-1 or DEN-4 h-Grp-2 and DEN-4 h-Cluster-1, DEN-4 h-Cluster-2 or DEN-4 h-Cluster-3 showed a dose-dependent increase ranging from 2-fold to more than 64-fold [*Bax*, *Btg2*, *Ccng1*, *Ccng2*, *Cdkn1a*, *Cyp4a10*, *Cyp21a1*, *Fos*, *Gadd45b*, *Gdf15*, *Hspb1*, *Hmox1*, *Hsp27*, *Igfbp1*, *Isg20l1*, *Jun*, *Mbd1*, *Mdm2*, *Myc*, *Net1*, *Plk2*, *Pmm1*, *Ppp1r3c*, *Rad52*, *Rcan1* and *Tubb2c*]. Two genes in DEN-4 h-Grp-4

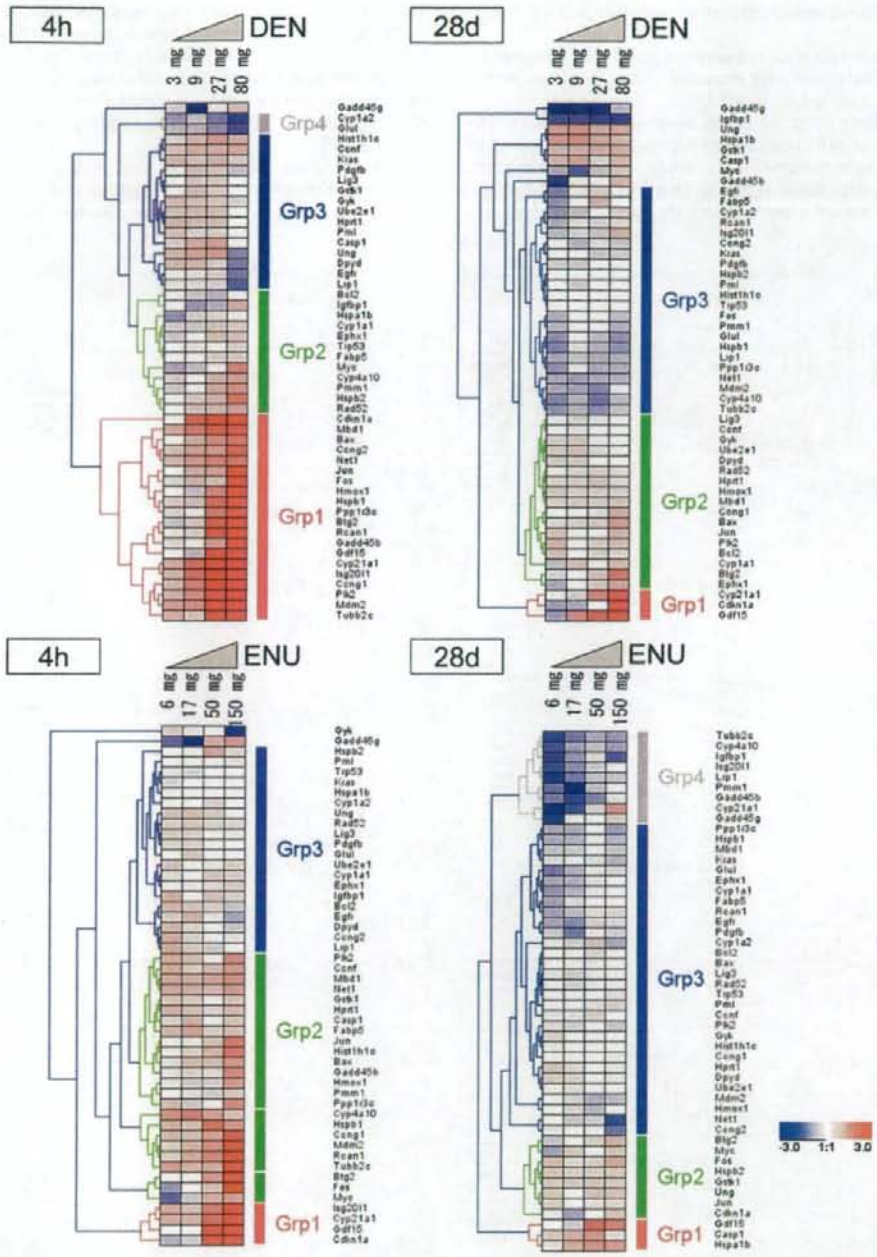

Fig. 2. Cluster analysis of gene expression after DEN and ENU treatment. The expression of 50 genes was clustered by hierarchical clustering after DEN or ENU treatment. Results of 4 h and 28 days were analyzed separately. The color displays show the $\log_2$ (expression ratio) as (1) red when the treatment sample is up-regulated relative to the control sample, (2) blue when the treatment sample is down-regulated relative to the control sample and (3) white when the $\log_2$ (expression ratio) is close to zero.

and DEN-4 h-Cluster-4 showed a dose-dependent decrease of less than 0.3-fold [*Cyp1a2* and *Glul*].

At 28 days, four genes in DEN-28 d-Grp-1 or DEN-28 d-Grp-2 and DEN-28 d-Cluster-1, which showed a dose-dependent increase at 4 h, also showed a dose-dependent increase by more than 2–4-fold [*Btg2*, *Cdkn1a*, *Cyp21a1* and *Gdf15*]. *Igfbp1* in the ungrouped group and DEN-28 d-Cluster-3 showed a dose-dependent decrease of less than 0.3-fold.

3.1.2. Identification of biologically relevant networks for DEN treatment

DEN numerical data of all 51 examined genes were analyzed by IPA, and 5 gene networks were extracted (Table 3). Five networks are also shown as bar graphs in Fig. 4.

For the 4 h time point, 35 genes were extracted in DEN-4 h-Network-1 (cancer, cell cycle and reproductive system disease); of these, 15 genes were examined in this study, and 11 of these genes showed a dose-dependent response [*Bax*, *Btg2*, *Ccng1*, *Cdkn1a*, *Gadd45b*, *Gdf15*, *Hspb1*, *Hspb2*, *Mdm2*, *Plk2* and *Pmm1*] (Fig. 4A, Network-1). Network-1 was a highly active network for DEN-4 h. *Trp53* and *Cdkn1a* appeared to be core genes in DEN-4 h-Network-1. *Trp53* has 15 associations [*Bax*, *Btg2*, *Casp1*, *Ccng1*, *Cdkn1a*, *Gadd45 complex*, *Gdf15*, *Hist1h1c*, *Hspb1*, *Mdm2*, *Plk2*, *Pml*, *Pmm1*, *Pdgf* complex and *Caspase* complex], and *Cdkn1a* has 9 associations [*Trp53*, *Plk2*, *Pdgf complex*, *Gdf15*, *Gadd45b*, *Gadd45g*, *Mdm2*, *Caspase* complex and *Pml*].

DEN-4 h-Network-2 (cell cycle, DNA replication, recombination, repair and cell death) consisted of 35 genes, 15 of which were examined in this study; 11 of these genes showed a dose-dependent

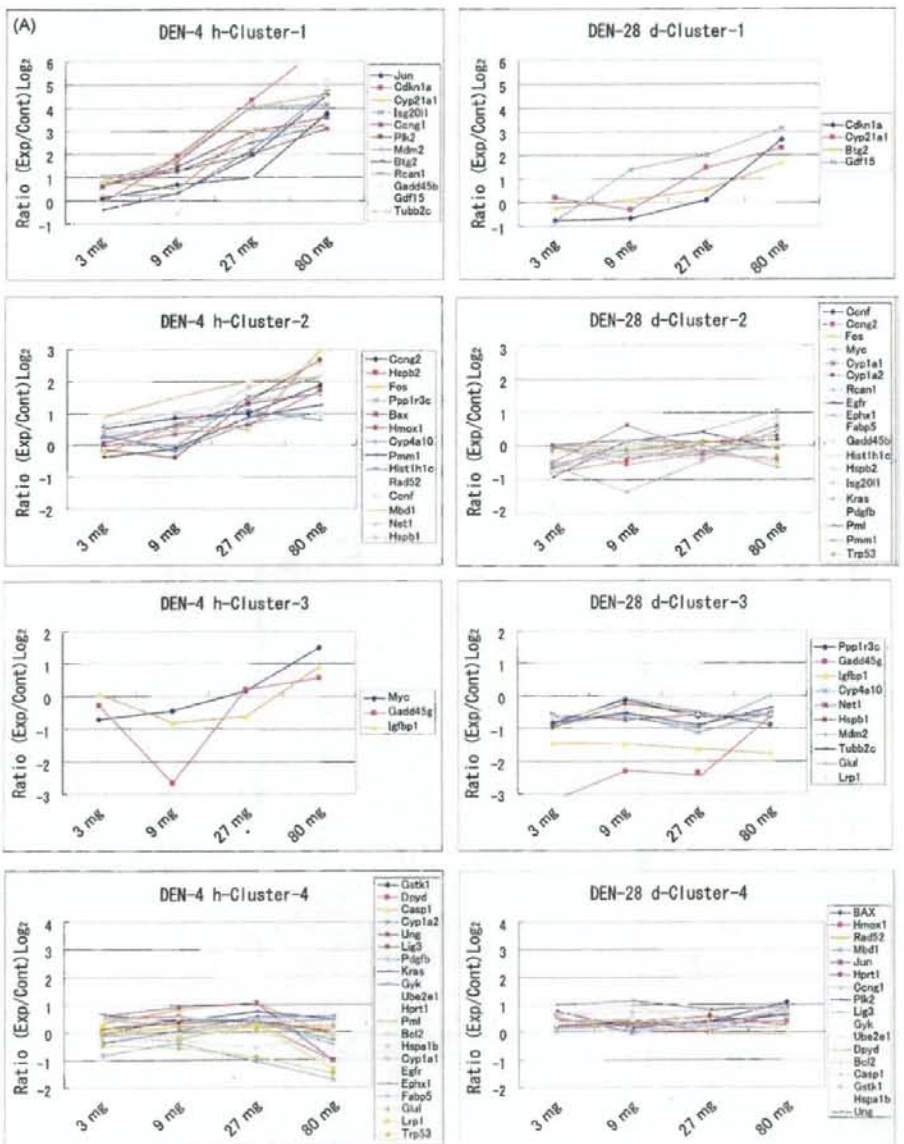

Fig. 3. Cluster analysis and dose-dependent expression pattern. The expression of 50 genes was clustered by *k*-means clustering after (A) DEN or (B) ENU treatment. Results of 4 h and 28 days were analyzed separately.

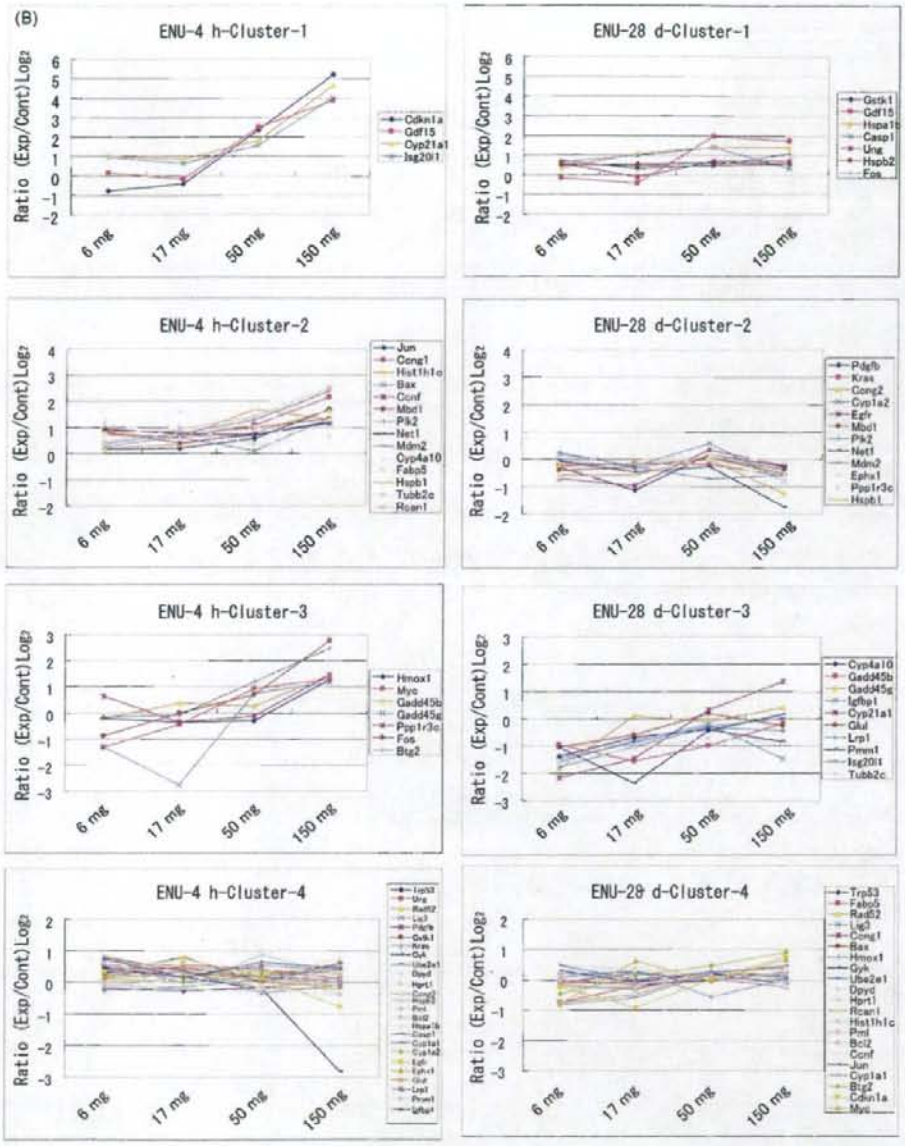

Fig. 3. (*Continued*).

response [*Ccng2*, *Cyp1a2*, *Cyp4a10*, *Cyp21a1*, *Gdf15*, *Glul*, *Igfbp1*, *Ppp1r3c Rad52*, *Rcan1* and *Tubb2c*] (Fig. 4A, Network-2). Network-2 was also a highly active network for DEN-4 h. *Il1b* and *Sp1* seemed to be core genes in DEN-4 h-Network-2. *Il1b* has five associations [*Gdf15*, *Fabp5*, *Rcan1*, *Igfbp1* and *Hprt1*], and *Sp1* has three associations [*Gdf15*, *Igfbp1* and *Cyp21a1*].

DEN-4 h-Network-3 (liver necrosis/cell death and hepatic system disease) consisted of 36 genes, 10 of which were examined in this study; 5 of these genes showed a dose-dependent response [*Fos*, *Hmox1*, *Jun*, *Myc* and *Net1*) (Fig. 4A, Network-3).

DEN-4 h-Network-4 (cell cycle, DNA replication, recombination, repair and cell death) consisted of 35 genes, 9 of which were examined in this study; 2 of these genes [*Isg20l1* and *Mbd1*] showed a dose-dependent response (Fig. 4A, Network-4).

DEN-4 h-Network-5 (cancer, drug metabolism and genetic disorder) consisted of two genes, neither of which showed a dose-dependent response in this study (Fig. 4A, Network-5).

For 28-day data, DEN-28 d-Network-1 consisted of the same genes and the same top functions as for DEN-4 h-Network-1 (Table 3(B)); however, a generally lower dose-dependent response

Table 3
Gene networks and their primary functions after DEN and ENU treatment.

Networks	Molecules in network	Top functions
(A) DEN 4 h		
1	Adaptor protein 2, Ahr-aryl hydrocarbon-*Arnt*, *Arf*, ***Bax***, ***Btg2***, *Casp1*, Caspase, *Cbp/p300*, ***Ccng1***, ***Cdkn1a***, *Creb*, Cyclin A, Cyclin E, *E2f*, *Erk1/2*, *Gadd45*, ***Gadd45b***, *Gadd45g*, ***Gdf15***, *Gsk3*, *Hist1h1c*, ***Hspb1***, ***Hspb2***, *Jun/Junb/Jund*, ***Mdm2***, *Mek1/2*, *Pak*, *Pdgf*, ***Plk2***, *Pml*, ***Pmm1***, *Pp2a*, *Rb*, *Stat*, *Trp53*	Cancer, Cell cycle, reproductive system disease
2	*Aatf*, *Aldh3a1*, *App*, beta-estradiol, *Ccne2*, ***Ccng2***, ***Cyp1a2***, ***Cpy21a1***, ***Cyp4a10***, *E2F1*, *Fabp5*, ***Gdf15***, *Gyk*, ***Glul***, *Hprt1*, *Hspa1b*, ***Igfbp1***, *Igfbp7*, *Il10*, *Il1b*, *Irf2*, *Klf10*, *MAZ*, *Meis1*, *Muc2*, ***Ppp1r3c***, ***Rad52***, ***Rcan1***, retinoic acid, *Scye1*, *Sp1*, *St8sia1*, *Tgm1*, *TopbpPT*, ***Tubb2c***	Cell cycle, DNA replication, recombination, and repair, cell death
3	*Akt*, *Ap1*, *Bcl2*, Calpain, *Egfr*, *Fgf*, ***Fos***, *Fos-Jun*, ***Hmox1***, *Ige*, *Il1*, *Jnk*, ***Jun***, *Kras*, *Lig3*, *Mapk*, *Mek*, *Mmp*, ***Myc***, ***Net1***, *P38*, *Mapk*, *Pdgf bb*, *Pdgfb*, *Pi3k*, *Pkc(s)*, *Pkg*, *Rar*, *Ras*, *Ras* homolog, *Rock*, *Rxr*, *Sos*, *Stat5a/b*, *Tgf* beta, *Vegf*	Cell death, hepatic system disease, liver necrosis/cell death
4	4-Phenylbutyric acid, *14-3-3*, Calmodulin, *Ccnf*, *Cdkn2a*, *Ck2*, *Culr1*, Cyclin D, *Cyp1a1*, *Ephx1*, *Hira*, Histone h3, *Hnrpa2b1*, *Hsp70*, *Hsp90*, *Hspa1b*, hydrogen peroxide, *Ifng*, *Irf2*, ***Isg20l1***, lipoxin A4, *Lrp1*, ***Mbd1***, *Mcm2*, *Mcm3*, *Meis1*, *Pdk1*, *Pka*, RNA polymerase II, *Ssrp1*, *Supt16h*, *Tp53inp1*, *Ube2e1*, Ubiquitin, *Ung*	Cell cycle, DNA replication, recombination, and repair, cell death
5	*Cdh3*, D *Dpyd*	Cancer, drug metabolism, genetic disorder
(B) DEN 28 d		
1	Adaptor protein 2, Ahr-aryl hydrocarbon-*Arnt*, *Arf*, *Bax*, ***Btg2***, *Casp1*, Caspase, *Cbp/p300*, *Ccng1*, ***Cdkn1a***, *Creb*, Cyclin A, Cyclin E, *E2f*, *Erk1/2*, *Gadd45*, *Gadd45b*, *Gadd45g*, ***Gdf15***, *Gsk3*, *Hist1h1c*, *Hspb1*, *Hspb2*, *Jun/Junb/Jund*, *Mdm2*, *Mek1/2*, *Pak*, *Pdgf*, *Plk2*, *Pml*, *Pmm1*, *Pp2a*, *Rb*, *Stat*, *Trp53*	Cancer, cell cycle, reproductive system disease
2	*Aatf*, *Aldh3a1*, *App*, beta-estradiol, *Ccng2*, *Cyp1a2*, ***Cyp21a1***, *Cyp4a10* (includes EG:1579), *E2f1*, *Fabp5*, ***Gdf15***, *Gyk*, *Glul*, *Hrpt1*, *Hspa1b*, ***Igfbp1***, *Il10*, *Il1b*, *Klf10*, *Klk5*, *Maz*, *Meis1*, *Mr1e*, *Muc2*, *Nr4a3*, *Ppp1r3c*, *Rad52*, *Rcan1*, retinoic acid, *Scye1*, *Sp1*, *St8sia1*, *Tgm1*, *Topbp1*, *Tubb2c*	DNA replication, recombination, and repair, cell death, cell cycle
3	*Akt*, *Ap1*, *Bcl2*, Calpain, *Egfr*, *Fgf*, *Fos*, *Fos-Jun*, *Hmox1*, *Ige*, *Il1*, *Jnk*, *Jun*, *Kras*, *Lig3*, *Mapk*, *Mek*, *Mmp*, *Myc*, *Net1*, *P38 Mapk*, *Pdgf bb*, *Pdgfb*, *Pi3k*, *Pkc(s)*, *Pkg*, *Rar*, *Ras*, *Ras* homolog, *Rock*, *Rxr*, *Sos*, *Stat5a/b*, *Tgf* beta, *Vegf*	Cell death, hepatic system disease, liver necrosis/cell death
4	*14-3-3*, *Bag4*, Calmodulin, *Ccnf*, *Cdkn2a*, *Ck2*, *Cutl1*, *Cyp1a1*, *Dynlrb1*, *Ephx1*, *Hira*, Histone h3, *Hnrpa2b1*, *Hoxb9*, *Hsp70*, *Hsp90*, *Hspa1b*, hydrogen peroxide, *Ifng*, *Isg20l1*, *Lrp1*, *Mbd1*, *Meis1*, *Nol3*, *Pdk1*, *Pka*, *Ppfibp1*, RNA pol2-transcription factor, RNA polymerase II, *Smtn*, *Supt16h*, *Tp53inp1*, *Ube2e1*, Ubiquitin, *Ung*	Cellular development, cellular growth and proliferation, connective tissue development and function
5	*Cdh3*, *Dpyd*	Cancer, drug metabolism, genetic disorder
(C) ENU 4 h		
1	Adaptor protein 2, Ahr-aryl hydrocarbon-*Arnt*, *Arf*, ***Bax***, ***Btg2***, *Casp1*, Caspase, *Cbp/p300*, ***Ccng1***, ***Cdkn1a***, *Creb*, Cyclin A, Cyclin E, *E2f*, *Erk1/2*, *Gadd45*, ***Gadd45b***, *Gadd45g*, ***Gdf15***, *Gsk3*, ***Hist1h1c***, ***Hspb1***, *Hspb2*, *Jun/Junb/Jund*, ***Mdm2***, *Mek1/2*, *Pak*, *Pdgf*, ***Plk2***, *Pml*, *Pmm1*, *Pp2a*, *Rb*, *Stat*, *Trp53*	Cancer, cell cycle, reproductive system disease
2	*Aatf*, *Aldh3a1*, *App*, *Appbp1*, beta-estradiol, *Ccne2*, *Ccng2*, *Cyp1a2*, ***Cyp21a1***, ***Cyp4a10***, *E2f1*, ***Fabp5***, ***Gdf15***, *Gyk*, *Glul*, *Hprt1*, *Hdps1b*, *Igfbp1*, *Il10*, *Il1b*, *Klf10*, *Maz*, *Mis1*, *Muc2*, *Nr4a3*, ***Ppp1r3c***, *Rad52*, ***Rcan1***, retinoic acid, *Scye1*, *Sp1*, *St8sia1*, *Tgm1*, *Topbp1*, ***Tubb2c***	DNA replication, recombination, and repair, cell cycle, cell signaling
3	*Akt*, *Ap1*, *Bcl2*, Calpain, *Egfr*, *Fgf*, ***Fos***, *Fos-Jun*, ***Hmox1***, *Ige*, *IL1*, *Jnk*, ***Jun***, *Kras*, *Lig3*, *Mapk*, *Mek*, *Mmp*, ***Myc***, ***Net1***, *P38*, *Mapk*, *Pdgf bb*, *Pdgfb*, *Pi3k*, *Pkc(s)*, *Pkg*, *Rar*, *Ras*, *Ras* homolog, *Rock*, *Rxr*, *Sos*, *Stat5a/b*, *Tgf* beta, *Vegf*	Cell death, hepatic system disease, liver necrosis/cell death
4	4-phenylbutyric acid, *14-3-3*, Calmodulin, ***Ccnf***, *Cdkn2a*, *Ck2*, *Culr1*, Cyclin D, *Cyp1a1*, *Ephx1*, *Hira*, Histone h3, *Hnrpa2b1*, *Hsp70*, *Hsp90*, *Hspa1b*, hydrogen peroxide, *Ifng*, *Irf2*, ***Isg20l1***, lipoxin A4, *Lrp1*, ***Mbd1***, *Mcm2*, *Mcm3*, *Meis1*, *Pdk1*, *Pka*, RNA polymerase II, *Ssrp1*, *Supt16h*, *Tp53inp1*, *Ube2e1*, Ubiquitin, *Ung*	Cell cycle, DNA replication, recombination, and repair, cell death
5	*Cdh3*, *Dpyd*	Cancer, drug metabolism, genetic disorder
(D) ENU 28 d		
1	Adaptor protein 2, Ahr-aryl hydrocarbon-*Arnt*, *Arf*, *Bax*, *Btg2*, ***Casp1***, Caspase, *Cbp/p300*, *Ccng1*, *Cdkn1a*, *Creb*, Cyclin A, Cyclin E, *E2f*, *Erk1/2*, *Gadd45*, *Gadd45b*, *Gadd45g*, ***Gdf15***, *Gsk3*, *Hist1h1c*, *Hspb1*, ***Hspb2***, *Jun/Junb/Jund*, *Mdm2*, *Mek1/2*, *Pak*, *Pdgf*, *Plk2*, *Pml*, *Pmm1*, *Pp2a*, *Rb*, *Stat*, *Trp53*	Cancer, cell cycle, reproductive system disease
2	*Aatf*, Ahr-aryl hydrocarbon, *App*, *Appbp1*, beta-estradiol, *Ccng2*, *Cd68*, *Cdc45l*, *Cyp1a2*, *Cyp21a1*, *Cyp4a10*, *E2f1*, *Fabp5*, *Folr2*, ***Gdf15***, *Gyk*, *Glul*, *Hprt1*, ***Hspa1b***, *Igfbp1*, *Il10*, *Il1b*, *Klk5*, *Krt16*, *Nr4a3*, *Ppp1r3c*, *Rad52*, *Rcan1*, retinoic acid, *Rrs4x*, *Serpinb9*, *Sp1*, *TacstdA1*, *Tspo*, *Tubb2c*	Cell signaling, molecular transport, small molecule biochemistry
3	*Akt*, *Ap1*, *Bcl2*, Calpain, *Egfr*, *Fgf*, ***Fos***, *Fos-Jun*, *Hmox1*, *Ige*, *IL1*, *Jnk*, *Jun*, *Kras*, *Lig3*, *Mapk*, *Mek*, *Mmp*, *Myc*, ***Net1***, *P38*, *Mapk*, *Pdgf bb*, *Pdgfb*, *Pi3k*, *Pkc(s)*, *Pkg*, *Rar*, *Ras*, *Ras* homolog, *Rock*, *Rxr*, *Sos*, *Stat5a/b*, *Tgf* beta, *Vegf*	Cell death, hepatic system disease, liver necrosis/cell death
4	*14-3-3*, *Aco1*, *Asf1b*, *Bag4*, Calmodulin, *Ccnf*, *Cdkn2a*, *Ck2*, *Cyp1a1*, *Dynlrb1*, *Ephx1*, *Hira*, Histone h3, *Hosb9*, *Hsp70*, *Hsp90*, ***Hspa1b***, hydrogen peroxide, *Ifng*, *Isg20l1*, *Lamp1*, *Lrp1*, *Mbd1*, *Nol3*, *Pka*, *Ppfibp1*, RNA pol2-transcription factor, RNA polymerase II, *Rpl21*, *Smtn*, *Sncg*, *Supt16h*, *Ube2e1*, Ubiquitin, ***Ung***	Cellular development, cellular growth and proliferation, connective tissue development and function
5	*Cdh3*, *Dpyd*	Cancer, drug metabolism, genetic disorder

Biologically relevant networks extracted by IPA are shown for gene expression data after (A) DEN-4 h, (B) DEN-28 d, (C) ENU-4 h or (D) ENU-28 d treatment. Bold underlined genes show dose-dependent expression. Thin underlined genes are genes examined in the present study. *Pdgf bb* in Network-3 means *Pdgf* groups of *Pdgfa*, *Pdgfb*, *Pdgfc* and *Pdgfd*. *Hsp70* in Network-4 means *Hsp* groups of *Hspa14 hspa1a*, *Hspa1b*, *Hspa11*, *Hspa2*, *Hspa4 hspa5*, *Hspa6*, *Hspa7*, *Hspa8*, and *Hspa9*.

was observed, and only *Btg2*, *Cdkn1a* and *Gdf15* showed a dose-dependent increase (Fig. 4A, Network-1). DEN-28 d-Network-2 included several different genes from those in DEN-4 h-Network-2 but had the same primary functions as for DEN-4 h-Network-2, and *Cyp21a1*, *Gdf15* and *Igfbp1* exhibited dose-dependency (Fig. 4A, Network-2). DEN-28 d-Network-3 consisted of the same genes and the same primary functions as for DEN-4 h-Network-3; however, no genes showed dose-dependency (Fig. 4A, Network-3). DEN-28 d-Network-4 contained a few different genes and primary functions from those of DEN-4 h-Network-4, but no genes showed a dose

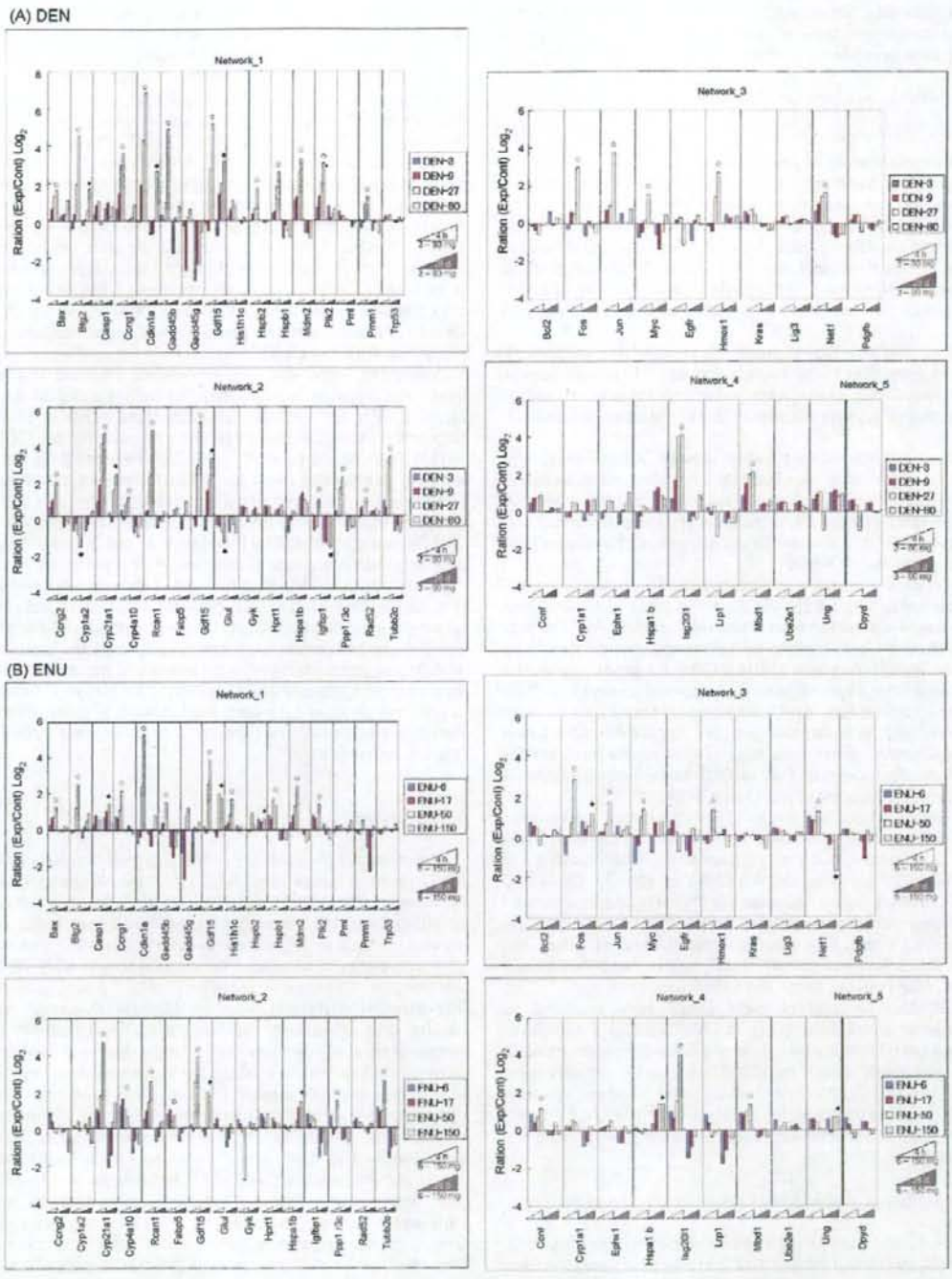

Fig. 4. Dose-dependent gene expression in each network based on different time points. The ratio values (log_2) of genes in each network are shown as bar graphs for DEN treatment (A) or ENU treatment (B). ○ shows a dose-dependent increase at 4 h, ♦ shows a dose-dependent increase at 28 days and ● shows a dose-dependent decrease.

response. DEN-28 d-Network-5 consisted of the same genes and the same top functions as those of DEN-4 h-Network-5, with no genes showing dose-dependency in this study (Fig. 4A, Network-5).

3.2. Dose-dependent alteration of gene expression induced with ENU

3.2.1. Clustering analysis for gene expression

Unsupervised hierarchical clustering results are shown in Fig. 2. The clustering presented three groups (ENU-4 h-Grp-1 to ENU-4 h-Grp-3) and two ungrouped genes for the 4 h time point after administration and four groups (ENU-28 d-Grp-1 to ENU-28 d-Grp-4) for the 28-day time point after administration. As unsupervised hierarchical clustering was performed on 4 h and 28-day data separately, group member genes were different between these two groups.

All four ENU-4 h-Grp-1 genes showed a dose-dependent increase by more than 16–32-fold 4 h after administration. Twenty-four ENU-4 h-Grp-2 genes were suggested to have a gradual dose-dependent increase of less than that of the expression in ENU-4 h-Grp-1.

All three ENU-28 d-Grp-1 genes showed a dose-dependent increase by more than two-fold 28 days after administration. Eight ENU-28 d-Grp-2 genes were suggested to have a gradual dose-dependent increase of less than that of the expression in ENU-28 d-Grp-1. *Net1* in ENU-28 d-Grp-3 showed a dose-dependent decrease of less than 0.3-fold.

Unsupervised *k*-means clustering results are shown in Fig. 3B. In the same way as for DEN, we classified these genes into four clusters based on hierarchical clustering results. For 4 h, four ENU-4 h-Cluster-1 genes exhibited a dose-dependent increase by more than 16-fold. Fourteen ENU-4 h-Cluster-2 genes exhibited a gradual dose-dependent increase as compared to genes in ENU-4 h-Cluster-1. Seven ENU-4 h-Cluster-3 genes showed an increase as a whole, with some atypical features. For 28-day data, seven ENU-28 d-Cluster-1 genes were suggested to have a tendency for a dose-dependent increase. *Net1* in ENU-28 d-Cluster-2 showed a dose-dependent decrease of less than 0.3-fold.

Two kinds of clustering results of ENU treatment are summarized as follows. A total of 29 genes showed a dose-dependent increase or decrease at 4 h or 28 days after administration. For 4 h, a total of 24 genes in ENU-4 h-Grp-1 or ENU-4 h-Grp-2 and ENU-4 h-Cluster-1, ENU-4 h-Cluster-2 or ENU-4 h-Cluster-3 showed a dose-dependent increase ranging from 2-fold to more than 32-fold [*Bax, Btg2, Ccng1, Ccnf, Cdkn1a, Cyp4a10, Cyp21a1, Fabp5, Fos, Gadd45b, Gdf15, Hist1h1c, Hmox1, Hspb1, Isg20l1, Jun, Mbd1, Mdm2, Myc, Net1, Plk2, Ppp1r3c, Rcan1* and *Tubb2c*].

For 28 days, a total of eight genes were classified as dose–response genes. Four genes in ENU-28 d-Grp-1, ENU-28 d-Grp-2, and ENU-28 d-Cluster-1 showed a dose-dependent increase of more than 2-fold [*Casp1, Fos, Gdf15* and *Hspa1b*]. Another three genes in ENU-28 d-Grp2 and ENU-28 d-Cluster-1 showed less than a two-fold increase [*Gstk1, Hspb2* and *Ung*]. *Net1* in ENU-28 d-Grp-3 and ENU-28 d-Cluster-2 showed a dose-dependent decrease of less than 0.3-fold.

3.2.2. Identification of biologically relevant networks for ENU treatment

ENU numerical data for all 51 examined genes were also analyzed by IPA for 4 h and 28-day data, and five gene networks were extracted (3). In total, the gene expression pattern for ENU was similar to the pattern for DEN; however, some differences were observed.

For 4 h, ENU-4 h-Network-1 consisted of the same genes and the same top functions as for DEN-4 h-Network-1, and 10 of these genes showed a dose-dependent increase [*Bax, Btg2, Ccng1, Cdkn1a, Gadd45b, Gdf15, Hist1h1c, Hspb1, Mdm2* and *Plk2*] (Fig. 4B, Network-1). Network-1 was the most active network for ENU-4 h. ENU-4 h-Network-2 (DNA replication, recombination, repair, cell cycle and cell signaling) included a different primary function from that of DEN-4 h-Network-2 and a few different genes from those for DEN, and seven genes showed a dose-dependent increase [*Cyp21a1, Cyp4a10, Fabp5, Gdf15, Ppp1r3c, Rcan1* and *Tubb2c*] (Fig. 4B, Network-2). ENU-4 h-Network-3 consisted of the same genes and the same top functions as those for DEN-4 h-Network-3, and five genes showed a dose-dependent increase [*Fos, Hmox1, Jun, Myc* and *Net1*] (Fig. 4B, Network-3). ENU-4 h-Network-4 also consisted of the same genes and the same top functions as those for DEN, and three genes showed a dose-dependent increase [*Ccnf, Isg20l1* and *Mbd1*] (Fig. 4B, Network-4). ENU-4 h-Network-5 consisted of the same genes and the same top functions as those for DEN-4 h-Network-5, but no genes showed a dose–response in this study (Fig. 4B, Network-5).

Network-1, Network-3 and Network-5 consisted of common genes and common top functions for both 4 h and 28 days and for both DEN and ENU. For 28 days, three genes in ENU-28 d-Network-1 showed a dose-dependent increase [*Casp1, Gdf15* and *Hspb2*] (Fig. 4B, Network-1). ENU-28 d-Network-2 included 10 different genes from those for ENU-4 h-Network-2 and had different top functions (cell signaling, molecular transport and small molecule biochemistry) from those of DEN-4 h-Network-2, DEN-28 d-Network-2 and ENU-4 h-Network-2, and 2 genes showed a dose-dependent increase [*Gdf15 and Hspa1b*] (Fig. 4B, Network-2). *Fos* and *Net1* in ENU-28 d-Network-3 showed a dose–response (Fig. 4B, Network-3). ENU-28 d-Network-4 (Table 2D) included different primary functions (cellular development, cellular growth, proliferation and connective tissue development and function) and 10 different genes from ENU-4 h-Network-4; two genes showed a dose–response [*Hspab1* and *Ung*]. ENU-28 d-Network-5 consisted of the same genes and the same top functions as those of DEN-4 h-Network-5, while no genes showed a dose–response in this study (Fig. 4A, Network-5).

4. Discussion

We examined the dose-dependency of gene expression changes for 51 genes in mouse liver treated with two *N*-nitroso genotoxic hepatocarcinogens, DEN and ENU, by qPCR at early times after administration. We selected 51 candidate genes based on our previous results of Affymetrix GeneChip Mu74AV2 and original DNA microarray of samples after treatment with DEN, dimethylnitrosamine, dipropylnitrosamine, ENU, *o*-aminoazotoluene, 7,12-dimethylbenz[*a*]anthracene, dibenzo[*a,l*]pyrene, phenobarbital and ethanol in our JEMS/MMS/Toxicogenomics group collaborative study. Because only a single dose was used for each chemical in the previous study, we examined dose-dependency in gene expression changes in this study using two representative chemicals. We showed distinct dose-dependency of gene expression changes induced by DEN and ENU; these changes associated with cancer, cell cycle arrest, DNA replication, recombination, repair and cell death not only at 4 h, but also, for some, at 28 days after administration. Similar gene expression changes between DEN and ENU were characteristic. Twenty-one genes exhibited a distinct dose-dependent increase at 4 h for both carcinogens [*Bax, Btg2, Ccng1, Cdkn1a, Cyp4a10, Cyp21a1, Fos, Gadd45b, Gdf15, Hmox1, Hspb1, Isg20l1, Jun, Mbd1, Mdm2, Myc, Net1, Plk2, Ppp1r3c, Rcan1* and *Tubb2c*], although the gene expression changed after ENU was generally weaker relative to that after DEN. The results were consistent with a previous report that showed more DNA lesions with DEN than with ENU a few hours after administration [6]. Only *Gdf15* showed a dose-dependent increase at 28 days for

both carcinogens. An additional seven different genes for DEN and eight genes for ENU also showed dose-dependency. *Ccng2*, *Hspb2*, *Igfbp1*, *Pmm1* and *Rad52* showed a dose-dependent increase and *Cyp1a2* and *Glul* showed a dose-dependent decrease 4 h after administration only with DEN. *Btg2*, *Cdkn1a* and *Cyp21a1* showed a dose-dependent increase 28 days after administration only with DEN and these genes also showed a dose–response at 4 h. *Ccnf*, *Fabp5* and *Hist1h1c* showed a dose-dependent increase 4 h after administration only with ENU. *Casp1*, *Fos*, *Gstk1*, *Hspa1b*, *Hspb2* and *Ung* showed a dose-dependent increase 28 days after administration only with ENU. *Ccnf* in DEN-4 h and *Bax* and *Ephx1* in DEN-28 d showed equivocal changes. We only observed several dose-dependent decreases in expression of genes [*Cyp1a2*, *Glul*, *Igfbp1* and *Net1*] after DEN and ENU in the present experimental conditions.

In the previous study [10], gene expression changes in number and degree were observed to peak at 4 h after administration and were lower at 20 h, 14 and 28 days. In the present study, we investigated the gene expression pattern at two different time points: 4 h, during production of many DNA lesions, and 28 days, during fixing of mutations [6]. We expected to observe the earliest and most varied effects in many cells in the liver, including DNA lesions, 4 h after administration. It was presumed that most of the DNA-damaged cells would be repaired, that some of the damaged cells would die and that only a few cells would progress to carcinogenesis. We reasoned that it would be useful to examine the earliest various effects to understand the potential gene-altering ability of carcinogens. The second time point, 28 days, is the time by which most mutations are fixed, the remainder of which would be related to carcinogenesis. We expected to observe gene expression changes which would reflect the effects of mutation at 28 days. The role of genes with altered expression might be different even if expression of the same gene was changed at 4 h and 28 days.

In addition, we examined gene networks using IPA to clarify interactions between genes with altered expression. IPA identified five networks of genes regulated at 4 h after DEN and ENU treatment (Table 3 and Fig. 4). As for DEN, 11 dose-dependent genes [*Bax*, *Btg2*, *Ccng1*, *Cdkn1a*, *Gadd45b*, *Gdf15*, *Hspb1*, *Hspb2*, *Mdm2*, *Plk2* and *Pmm1*] belonged to Network-1 (cancer and cell cycle) and the other 11 dose-dependent genes [*Ccng2*, *Cyp1a2*, *Cyp4a10*, *Cyp21a1*, *Gdf15*, *Glul*, *Igfbp1*, *Ppp1r3c Rad52*, *Rcan1* and *Tubb2c*] belonged to Network-2 (cell cycle, cell death, DNA replication, recombination and repair). In detail, *Gdf15* was extracted in both Network-1 and Network-2. As for ENU, 10 dose-dependent genes [*Bax*, *Btg2*, *Ccng1*, *Cdkn1a*, *Gadd45b*, *Gdf15*, *Hist1h1c*, *Hspb1*, *Mdm2* and *Plk2*] belonged to the same Network-1 and 7 dose-dependent genes [*Cyp21a1*, *Cyp4a10*, *Fabp5*, *Gdf15*, *Ppp1r3c*, *Rcan1* and *Tubb2c*] belonged to a different Network-2 (DNA replication, recombination and repair, and cell cycle and cell signaling). *Hspb2* and *Pmm1* showed dose–responses only in DEN-4 h-Network-1 and *Hist1h1c* showed a dose–response only in ENU-4 h-Network-1. [Cell death] in DEN-4 h-Network-2 was replaced with [Cell signaling] in ENU-4 h-Network-2. *Ccng2*, *Cyp1a2*, *Glul*, *Igfbp1* and *Rad52* showed dose–responses only in DEN-4 h-Network-2 and *Fabp5* showed a dose–response only in ENU-4 h-Network-2. This difference in Network-2 was the most remarkable difference between the effects of DEN and ENU in the present study. The top functions of Network-1 and Network-2 were characteristic networks for DEN-4 h and ENU-4 h, being typical of carcinogenic compounds. As for 28 days, IPA also identified five networks of genes, however, only a few genes showed a dose–response with DEN and ENU. As for DEN, three dose-dependent genes [*Btg2*, *Cdkn1a* and *Gdf15*] belonged to Network-1 and two genes [*Cyp21a1* and *Gdf15*] belonged to Network-2. As for ENU, three dose-dependent genes [*Casp1*, *Gdf15* and *Hspb2*] belonged to Network-1, [*Gdf15* and *Hspa1b*] belonged to Network-2, [*Fos* and *Net1*] belonged to Network-3 and [*Hspa1b* and *Ung*] belonged to Network-4. The present results suggested similar functions for *N*-nitroso carcinogens DEN and ENU, with several differences. We have examined effects of other genotoxic and non-genotoxic carcinogens in mouse liver at 4 h and have generated various networks for various carcinogens (unpublished).

We showed that Network-1 was associated with cancer and the cell cycle. To understand more detailed functions, we examined a major canonical pathway for each network. A major canonical pathway in Network-1 was *p53* signaling. The increase of *Cdkn1a*, *Ccng1* and *Gadd45* demonstrated cell cycle arrest. The expression pattern (Fig. 4) at 4 h showed that cell cycle arrest would proceed, to then be released by day 28. Both *p53* and *Bax* were associated with initiation of apoptosis.

In the same way, a major canonical pathway in Network-2 was aryl hydrocarbon receptor signaling [14]. Furthermore, aryl hydrocarbon receptor signaling as an adaptive response was manifested as the induction of xenobiotic metabolizing enzymes; *Cyp1a2*, *Cyp21a1* and *Cyp4a10* take part in this pathway. *Cyp21a1* also takes part in biosyntheses of steroid hormones [15]. Inflammation of the liver is controlled at 28 days after administration because steroid hormones function to suppress inflammation.

Growth/differentiation factor-15 (*Gdf15*) was the only gene whose expression increased at 4 h and 28 days of both DEN and ENU and belonged to Network-1 and Network-2 at 4 h and 28 days of DEN and ENU. *Gdf15* is a divergent Tgf-beta family member that is expressed following liver injury and carcinogen exposure [16]. *Gdf15* in liver is rapidly and dramatically up-regulated following various surgical and chemical treatments that cause acute liver injury and regeneration [17].

A major canonical pathway in Network-3 was platelet-derived growth factor (*Pdgf*) signaling. *Pdgfb*, *Kras*, *Jun*, *Fos* and *Myc* may be associated with *Pdgf* signaling. In this canonical pathway, *Pdgfb* phosphorylates other proteins and activates the downstream genes *Kras*, *Jun*, *Fos* and *Myc* [18–21], one reason why *Pdgfb* expression did not change significantly (Fig. 3A, Cluster-4).

Our results show that most differentially expressed genes at 4 h and 28 days exhibited a dose–response. Only a few genes, *Dpyd*, *Egfr*, *Lrp1* and *Ung* for DEN at 4 h; *Gyk* for ENU at 4 h; and *Ccng2* for ENU at 28 days showed atypical gene expression changes at the highest dose. These changes may be toxicity-related. *Dpyd* is associated with pyrimidine metabolism. *Egfr* is associated with cell proliferation. *Lrp* plays a clear protective role in atherogenesis. *Ung* is associated with DNA repair. Their decrease may show the loss of cell maintenance because hepatocytes will have received much lethal damage at the highest dose. *Gyk* is associated with xenobiotic metabolism signaling. It has been reported that glycerol kinase deficiency is involved in lipid metabolism, carbohydrate metabolism, and insulin signaling [22]. Indeed, it has been reported that type 2 diabetes is caused by ENU but not by DEN [23]. Unlike classical cyclins that promote cell cycle progression, cyclin G2 blocks cell cycle entry. The decrease of *Ccng2* mRNA may promote cell cycle progression.

Previously, we reported differential gene expression induced by two *N*-nitroso genotoxic hepatocarcinogens, DEN and dipropylnitrosamine (DPN) as compared to phenobarbital and ethanol in mouse liver examined with an original oligonucleotide microarray and qPCR [10]. We observed 11 differentially expressed genes 4 h after administration, including 7 tumor suppressor *Trp53* target genes, *Bax*, *Ccng1*, *Cdkn1a*, *Hspb2*/*Hsp27*, *Jun*, *Mdm2*, and *Plk2*/*Snk*; the other genes were *Ccnf*, *Hmox1*, *Mbd1*, and *Rad52*. Furthermore, some degree of differential gene expression of *Ccng1*, *Cdkn1a* and *Plk2*/*Snk* was observed 28 days after administration. In the present study, we selected 51 candidate genes (Table 1) based on our original DNA microarray and Affymetrix GeneChip Mu74AV2 data (not published) on seven genotoxic carcinogens, phenobarbital and ethanol. The present results show that 28 genes for

DEN and 29 genes for ENU exhibited dose-dependent differential expression. Differential gene expression was observed commonly at least for *Bax*, *Ccng1*, *Cdkn1a*, *Hmox1*, *Jun*, *Mbd1*, *Mdm2* and *Plk2* with these three *N*-nitroso carcinogens (DEN, DPN and ENU). As we expanded qPCR analysis from 14 genes in the previous study [10] to 51 genes in the present study, we could show complex gene networks by IPA. Twenty genes, *Btg2*, *Casp1*, *Ccng2*, *Cyp4a10*, *Cyp21a1*, *Ephx1*, *Gadd45b*, *Gdf15*, *Glul*, *Gstk1*, *Hspa1b*, *Hspb1*, *Igfbp1*, *Isg20l1*, *Net1*, *Pmm1*, *Ppp1r3c*, *Rcan1*, *Tubb2c* and *Ung*, which showed dose–responses in the present study, were newly examined.

We examined only pooled materials from five mice in the present study. However, we already reported that at least five genes (*Gapdh*, *Jun*, *Ccng1*, *Hspb2*/*Hsp27* and *Rad52*) exhibited only small inter-individual mouse gene expression variation [10] with DEN treatment after 4 h and 28 days. Additional study showed that *Bax*, *Hmox1*, *Mbd1*, *Mdm2* and *Plk2* also exhibited only small inter-individual gene expression variation with DEN treatment at 4 h and 28 days (unpublished data).

We will continue further studies on other types of chemicals for characterizing mutagenic and carcinogenic compounds; these data will be useful for chemical risk assessment and for furthering our understanding of the underlying biological processes.

Conflict of interest

We have not any conflicting interest include employment, consultancies, stock ownership, honoraria, paid expert testimony, patent applications/registrations, and grants or other funding.

Acknowledgements

This work was partly supported by KAKENHI (18310047) (C. Furihata, T. Watanabe and T. Suzuki), The Ministry of Education, Culture, Sports, Science and Technology, Japan and a High-Tech Research Center project for private universities with a matching fund subsidy from The Ministry of Education, Culture, Sports, Science and Technology, Japan (C. Furihata).

References

[1] B.A. Diwan, H. Meier, Carcinogenic effects of a single dose of diethylnitrosamine in three unrelated strains of mice: genetic dependence of the induced tumor types and incidence, Cancer Lett. 1 (1976) 249–253.
[2] A.P. Kyriazis, S.D. Vesselinovitch, Transplantability and biological behavior of mouse liver tumors induced by ethylnitrosourea, Cancer Res. 33 (1973) 332–338.
[3] J.A. Swenberg, M.C. Dyroff, M.A. Bedell, J.A. Popp, N. Huh, U. Kirstein, M.F. Rajewsky, O4-ethyldeoxythymidine, but not O6-ethyldeoxyguanosine, accumulates in hepatocyte DNA of rats exposed continuously to diethylnitrosamine, Proc. Natl. Acad. Sci. U.S.A. 81 (1984) 1692–1695.
[4] J.L. Yang, P.C. Lee, S.R. Lin, J.G. Lin, Comparison of mutation spectra induced by N-ethyl-N-nitrosourea in the hprt gene of Mer+ and Mer– diploid human fibroblasts, Carcinogenesis 15 (1994) 939–945.
[5] T. Suzuki, M. Hayashi, T. Sofuni, Initial experiences and future directions for transgenic mouse mutation assays, Mutat. Res. 307 (1994) 489–494.
[6] E.J. Mientjes, A. Luiten-Schuite, E. van der Wolf, Y. Borsboom, A. Bergmans, F. Berends, P.H. Lohman, R.A. Baan, J.H. van Delft, DNA adducts, mutant frequencies, and mutation spectra in various organs of lambda lacZ mice exposed to ethylating agents, Environ. Mol. Mutagen. 31 (1998) 18–31.
[7] J.F. Waring, R.A. Jolly, R. Ciurlionis, P.Y. Lum, J.T. Praestgaard, D.C. Morfitt, B. Buratto, C. Roberts, E. Schadt, R.G. Ulrich, Clustering of hepatotoxins based on mechanism of toxicity using gene expression profiles, Toxicol. Appl. Pharmacol. 175 (2001) 28–42.
[8] M.J. Bartosiewicz, D. Jenkins, S. Penn, J. Emery, A. Buckpitt, Unique gene expression patterns in liver and kidney associated with exposure to chemical toxicants, J. Pharmacol. Exp. Ther. 297 (2001) 895–905.
[9] M. Provenzano, S. Mocellin, Complementary techniques: validation of gene expression data by quantitative real time PCR, Adv. Exp. Med. Biol. 593 (2007) 66–73.
[10] T. Watanabe, K. Tobe, Y. Nakachi, Y. Kondoh, M. Nakajima, S. Hamada, C. Namiki, T. Suzuki, S. Maeda, A. Tadakuma, M. Sakurai, Y. Arai, A. Hyogo, M. Hoshino, T. Tashiro, H. Ito, H. Inazumi, Y. Sakaki, H. Tashiro, C. Furihata, Differential gene expression induced by two genotoxic *N*-nitroso carcinogens, phenobarbital and ethanol in mouse liver examined with oligonucleotide microarray and quantitative real-time PCR, Gene Environ. 29 (2007) 115–127.
[11] K. Sekihashi, A. Yamamoto, Y. Matsumura, S. Ueno, M. Watanabe-Akanuma, F. Kassie, S. Knasmüller, S. Tsuda, Y.F. Sasaki, Comparative investigation of multiple organs of mice and rats in the comet assay, Mutat. Res. 517 (2002) 53–75.
[12] S. Madle, S.W. Dean, U. Andrae, G. Brambilla, B. Burlinson, D.J. Doolittle, C. Furihata, T. Hertner, C.A. McQueen, H. Mori, Recommendations for the performance of UDS tests in vitro and in vivo, Mutat. Res. 312 (1994) 263–285.
[13] A. Sturn, J. Quackenbush, Z. Trajanoski, Genesis: Cluster analysis of microarray data, Bioinformatics 18 (2002) 207–208.
[14] D.W. Kim, L. Gazourian, S.A. Quadri, R. Romieu-Mourez, D.H. Sherr, G.E. Sonenshein, The RelA NF-kappaB subunit and the aryl hydrocarbon receptor (AhR) cooperate to transactivate the Myc promoter in mammary cells, Oncogene 19 (2000) 5498–5506.
[15] J. Gonçalves, A. Friães, L. Moura, Congenital adrenal hyperplasia: focus on the molecular basis of 21-hydroxylase deficiency, Expert Rev. Mol. Med. 9 (2007) 1–23.
[16] T.A. Zimmers, X. Jin, J.C. Gutierrez, C. Acosta, I.H. McKillop, R.H. Pierce, L.G. Koniaris, Effect of in vivo loss of GDF-15 on hepatocellular carcinogenesis, J. Cancer Res. Clin. Oncol. 134 (2008) 753–759.
[17] E.C. Hsiao, L.G. Koniaris, T. Zimmers-Koniaris, S.M. Sebald, T.V. Huynh, S.J. Lee, Characterization of growth-differentiation factor 15, a transforming growth factor beta superfamily member induced following liver injury, Mol. Cell. Biol. 20 (2000) 3742–3751.
[18] S. Svegliati, R. Cancello, P. Sambo, M. Luchetti, P. Paroncini, G. Orlandini, G. Discepoli, R. Paterno, M. Santillo, C. Cuozzo, S. Cassano, E.V. Avvedimento, A. Gabrielli, Platelet-derived growth factor and reactive oxygen species (ROS) regulate Ras protein levels in primary human fibroblasts via ERK1/2. Amplification of ROS and Ras in systemic sclerosis fibroblasts, J. Biol. Chem. 280 (2005) 36474–36482.
[19] J.W. Tullai, M.E. Schaffer, S. Mullenbrock, S. Kasif, G.M. Cooper, Identification of transcription factor binding sites upstream of human genes regulated by the phosphatidylinositol 3-kinase and MEK/ERK signaling pathways, J. Biol. Chem. 279 (2004) 20167–20177.
[20] A.J. Kudla, M.L. John, D.F. Bowen-Pope, B. Rainish, B.B. Olwin, A requirement for fibroblast growth factor in regulation of skeletal muscle growth and differentiation cannot be replaced by activation of platelet-derived growth factor signaling pathways, Mol. Cell. Biol. 15 (1995) 3238–3246.
[21] P.A. Bromann, H. Korkaya, C.P. Webb, J. Miller, T.L. Calvin, S.A. Courtneidge, Platelet-derived growth factor stimulates Src-dependent mRNA stabilization of specific early genes in fibroblasts, J. Biol. Chem. 280 (2005) 10253–10263.
[22] L. Rahib, N.K. MacLennan, S. Horvath, J.C. Liao, K.M. Dipple, Glycerol kinase deficiency alters expression of genes involved in lipid metabolism, carbohydrate metabolism, and insulin signaling, Eur. J. Hum. Genet. 15 (2007) 646–657.
[23] A.A. Toye, L. Moir, A. Hugill, L. Bentley, J. Quarterman, V. Mijat, T. Hough, M. Goldsworthy, A. Haynes, A.J. Hunter, M. Browne, N. Spurr, R.D. Cox, A new mouse model of type 2 diabetes, produced by N-ethyl-nitrosourea mutagenesis, is the result of a missense mutation in the glucokinase gene, Diabetes 53 (2004) 1577–1583.